BIOSORPTION OF HEAVY METALS BY CITRUS FRUIT WASTE MATERIALS

By

Santosh Bramhadev Patil

RECOMMENDED:

Advisory Committee Chair

Chair, Department of Civil & Environmental Engineering

APPROVED:

John Aspnes
Dean, College of Engineering & Mines

Susan A. Henrichs
Dean of the Graduate School

January 7, 2005
Date

BIOSORPTION OF HEAVY METALS BY CITRUS FRUIT WASTE MATERIALS

A

THESIS

Presented to the Faculty

of the University of Alaska Fairbanks

in Partial Fulfillment of the Requirements

for the Degree of

MASTER OF SCIENCE

By

Santosh Bramhadev Patil, B.E.

Fairbanks, Alaska

December 2004

Abstract

Conventionally used processes for removing heavy metals from wastewater are usually either expensive, such as ion exchange, or inefficient, such as precipitation. An innovative technique that is both efficient and economical is biosorption, in which living and dead biomass can act as biosorbents through physical–chemical processes like ion exchange and micro-precipitation.

Pectin, a structural polysaccharide present in plant cell walls, is similar to alginate, a molecule that is often responsible for the high metal uptake by algae. Based on the structural similarity between alginate and pectin, it was expected that pectin rich bio-wastes may be as good a biosorbent material as brown algae. A comparison between different pectin-rich materials showed high stability and metal binding capacity of citrus peels. Sorption isotherms for citrus peels showed higher metal uptake capacity at pH 5 compared to pH 3. Kinetic studies revealed the time required to reach equilibrium for lemon fruit waste (0.177 mm) was 20 min while for larger particles the time increased to 30 min-60 min. For lemon fruit waste, the content and pK_a values of acidic groups were determined by using a pK_a spectrum technique. Isotherm modeling was carried out by using Langmuir isotherms and pH sensitive modeling.

Table of Contents

List of Figures

List of Tables

List of Appendices

Acknowledgements

I dedicate this work to my parents, sisters and their families, because without their support and love my journey to this country would have been impossible. I would like to offer my sincere thanks to my advisor Dr. Silke Schiewer for her constant support and guidance in my endeavor and for always welcoming new ideas. I am extremely thankful to my committee members Dr. Dan White and Dr. David Barnes for their valuable advice and support during the course of this project.

This research was supported by EPSCoR (Experimental Program to Stimulate Competitive Research), INE (Institute of Northern Engineering), and AWRA (American Water Resources Association) and their support is gratefully acknowledged. I thank Sunkist® for donating lemon fruit waste for this research. I am very thankful to Dr. D. Scott Smith of Wilfrid Laurier University, Canada for sending me Matlab® codes for the titration study. Last but not least I thank all of my friends here and in India for their help and encouragement.

Chapter 1

Introduction

1.1 Background

Heavy metals can be major toxic pollutants in marine, ground, and wastewater. Heavy metal contamination can occur due to mining activities and metal ore refining. The atmospheric deposition of heavy metals released in other parts of world is another contributing element that adds to heavy metal pollution. Heavy metals seep into the water supply and eventually enter into the food chain. The accumulation of heavy metals in the human body can be harmful to human health. The ill effects of accumulation of heavy metals have been studied extensively. For example, the bowhead whales, which are a source of food for many Native Alaskans, contain cadmium at levels that may be of concern for human health. Due to increasingly stringent regulations, new technologies to remove heavy metals from wastewater are in high demand.

Traditional methods like chemical precipitation, chemical oxidation or reduction, filtration, electrochemical treatment, membrane technology and ion exchange have been employed for heavy metal removal for decades. But these methods can be extremely expensive or inefficient, especially when the metals are dissolved in large volumes of solution at very low concentrations. A new technology called 'Biosorption' has emerged which uses dead (Cossich at al., 2002) or live biological materials (Pangnanelli et al., 2000) to recover heavy metals from contaminated wastewater.

The uptake of metal ions may occur by entrapment in the cell wall or uptake into the cell and subsequent attachment of the metal ions onto functional groups by ion exchange. Since this method of metal uptake does not involve any metabolic activity, it is called 'passive uptake'. Biosorbent materials like sea algae, crab shells, or sewage sludge are cheap, naturally occurring materials or industrial wastes. Atkinson et al. (1998) mainly focused on the feasibility and cost aspects of the biosorption process. The cost for commercially available alginate was found to be 7-12 times lower than that of synthetic ion exchange resins.

The effectiveness, availability, and the ease of desorbing of metals from the sorbent materials are prime attributes of the biosorption process. Micro-precipitation, complex formation, and ion exchange are the important mechanisms in the biosorption process. Factors like pH, size of biosorbent, ionic strength and temperature influence metal uptake by biosorbent materials.

It has been observed that alginate, which contains carboxyl groups, is responsible for metal uptake by brown algae (Chen and Wong 2001, Cossich et al., 2002 and Davis et al., 2001). The sorption performance of this type of algal biomass has been extensively studied. A polysaccharide which closely resembles alginate in structure is pectin. Kohn (1987) investigated the interactions between carboxyl groups present in pectin and divalent metal ions. Recent studies (Dronnet, 1996) have corroborated the removal of heavy metal ions by using sugar beet pulp, which is one of the prime sources of pectin.

The metal uptake by pectin rich biological materials may be due to similar mechanisms based on the structural similarity between alginate (present in algae) and pectin.

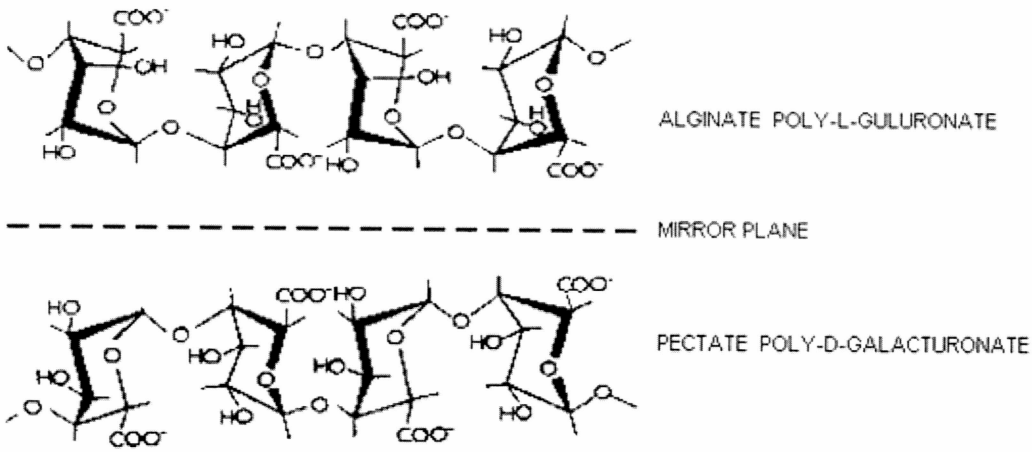

Figure 1.1: Structure of alginate and pectate (Genialab 2002)

Pectin is an anionic polysaccharide present primarily in cell walls and the intercellular matrix of higher plants. The important feature of pectin is the linear chain of α - (1-4) linked D-galacturonic acid.

Very few studies (Ajmal et al., 2000, Annadurai et al., 2003, Jumle et al., 2002, and Maranon and Sastre 1992) have been carried out to investigate the metal uptake capacities of pectin-rich waste materials from the fruit juice industry, such as orange peels, or apple residues, other fruit peels or pectin rich biological materials like ferns (Cohen-Shoel et al., 2002). No conspicuous research has been performed in the United States even though the USA produces large quantities of fruit juice industry waste. The

understanding of the biosorption process for pectin-rich fruit materials can be applied to economically utilize the fruit waste (high in pectin content). Fruit waste can be purchased at minimal cost and it is easily available everywhere. According to Vincent (2001), dried citrus peels for pectin production are sold for $300-600/short ton while cost of commercially used ion exchange resins ranges from $30,000-50,000/short ton. Developing countries like India, where the fruit waste is commonly disposed off, would particularly benefit from using low cost biosorbent materials for metal bearing waste stream treatment, which would otherwise be too expensive. The current research primarily studies pectin-rich citrus fruit materials to understand and evaluate their metal binding capacities.

1.2 Hypotheses

From prior research it is known that carboxyl groups are very effective in binding metal ions (as has been shown in the case of algae), and that large quantities of pectin, which is rich in carboxyl groups, occur in citrus peels. Correspondingly, this research investigated the following hypotheses:

- Citrus fruit waste is a high performance biosorbent with a good uptake capacity.
- Carboxyl groups, which are known to be effective in metal binding, are one of the major functional groups in citrus peels.
- Biosorption by citrus peels is a fast process and sorption kinetics is affected by mass transfer.

- Kinetic and equilibrium models previously used in other biosorption studies can be applied to fit citrus peel biosorption data.

1.3 Objectives of the study

The following objectives formed the basis of this investigation of the above hypotheses:

- Comparison between different pectin-rich fruit materials (commercially used for pectin extraction) and evaluation of the suitability of citrus peels for biosorption (hypothesis 1).
- Characterization of citrus biosorbent materials by potentiometric titration (hypothesis 2).
- Kinetic studies of the biosorbent material at different pH and for different particle sizes (hypothesis 3).
- Isotherm studies and modeling of the data (hypotheses 1, 2, and 4).

Chapter 2

Literature Review

There have been numerous studies carried out to characterize biosorbent materials by using potentiometric titration and to understand the metal uptake mechanism as well as different modeling approaches. The published work in this area is subdivided into four major categories:

- Biomass preparation, protonation and characterization (using potentiometric titration).
- Dynamics studies with modeling.
- Comparison of biosorbent materials and isotherm studies.
- Biosorption equilibrium modeling.

2.1 Biomass preparation, protonation and characterization

2.1.1 Preparation

Maranon and Sastre (1992) increased the structural stability of an agricultural waste obtained from apple juice processing and cider production. This was achieved by simple chemical treatment with phosphorus (V) oxychloride to introduce phosphate groups as a cross-linking agent, followed by protonation with hydrochloric acid (HCl). The cation exchange behavior under dynamic conditions was studied in glass columns. The

comparison between breakthrough and dynamic capacities of cross-linked and untreated biomass showed that breakthrough capacities of cross-linked fruit waste were 5-8 times higher than those of unmodified fruit waste.

Cohen-Shoel et al. (2002) treated *Azolla* biomass (containing 3-5% pectin) with methanol and HCl for 6 hours to obtain the methylated form of pectin. The Sr^{2+} binding capacity of methylated biomass was observed to be lower than that of untreated biomass, which indicated the blocking of carboxyl groups of pectin, participating in Sr^{2+} binding by *Azolla*. An increase in Sr^{2+} binding after alkaline treatment was attributed to demethylation of esterified carboxyl groups.

The current study used citrus fruit materials to investigate the biosorption process for pectin-rich fruit materials. As studies by Cohen-Shoel et al. (2002) suggested, the modification of *Azolla* biomass by demethylation increased the sorption capacity due to an increase of carboxyl groups. In the present work no modification was performed to save costs. Citrus peels generally feature pectin with a low degree of acetylation (Dronnet et al. 1996) so that further treatment was considered unnecessary. However, further investigation of modification of citrus fruit materials will be useful in future studies.

The brown seaweed *Sargassum* sp. (*Chromophyta*) used by Antunes et al. (2003) was harvested from the sea (Northeastern Coast of Brazil). Then it was extensively washed

with distilled water to remove particulate material from its surface and oven-dried at 343°K for 24 hours. One kg of biomass was sub-sampled for use in the experiments. Dried biomass was cut, ground in a mortar and pestle and then sieved. The fraction with 0.3-0.7 mm particle diameter was selected for use in the sorption test.

2.1.2 Protonation

Protonation of non-living biomass of *Sargassum* seaweed was performed by Yang and Volesky (1999) in their study of biosorption of uranium with seaweed. In the protonation process a batch of dry biomass with particle diameters equal to 1.0-1.4mm was pretreated with mineral acid to standardize the biomass by removing the light metals such as Ca^{2+}, Mg^{2+}, etc. The protonation was achieved by treating biomass with 0.1 N HCl (10 g of biomass / L) for 3 hours, which was followed by rinsing with de-ionized water in the same volume many times. The biomass was then dried for 12 hours in an oven at 40-60°C.

2.1.3 Characterization

Synytsya et al. (2003) examined the FT-Raman and FTIR (FT-Fourier Transform, IR-Infrared) spectra of pectic acid and potassium pectate as well as commercial citrus and sugar beet pectin. In the case of pectic acid and potassium pectate, the most intense Raman band at 2940/cm was assigned to the stretching of the C-H bonds of pyranoid ring carbons. The FTIR studies showed a 3600-3200/cm band which was attributed to the O-H

bonds of hydroxyl and bound water. The presence of C=O stretching of -COOH was confirmed in the case of both spectral studies (1740/cm for FT-Raman and 1762/cm for FTIR). The FT-Raman and FTIR spectra of sugar beet and citrus pectins indicated the presence of carboxyl groups in different forms of pectin, such as methylated pectin having a wave number of 1750/cm for FT-Raman spectra.

Lee et al. (1999) experimentally studied the methanol esterification of carboxyl groups of apple residue. The FTIR analysis on dried and protonated apple residue showed the presence of the C=O band (1700/cm) of carboxyl groups and the OH^- band (3400/cm) of phenolic groups. The effect of pH was investigated for Cu^{2+}, Cd^{2+} and Pb^{2+} adsorption on apple residue. The optimal pH range for cadmium sorption was 8-9.5. The decreased sorption capacity of esterified apple residue pectin was attributed to a decrease in free carboxyl groups.

Kohn (1987) succeeded in evaluating the interaction among different cations like Ca^{2+}, Cd^{2+}, Cu^{2+}, Pb^{2+}, Sr^{2+} and Zn^{2+} in their associations with carboxyl groups present in pectin by determining activity coefficients and the degree of association (defined as the portion of bound cations relative to their total initial amount in solution). The polymerization of oligoD-galactosyluronates (polymer present in pectin) was observed to affect the binding of cations. The study was carried out by first determining the activity coefficients of divalent cations in the presence of monomeric D-galactopyranuronic acid, which suggested the absence of a complex formation in the case of calcium ions, while

the same study showed stronger bond formations for other cations like Cd^{2+} and Cu^{2+}. An increase in the degree of polymerization of oligo-D-galactosyluronates was found to increase binding of all cations. The degree of association of divalent cations was proved to be another important parameter, which revealed that divalent metal cations are bound stoichiometrically (one cation per 2 carboxyl groups) by polymeric D-galacturonates as well as by pectin having different degrees of esterification. The intra-molecular bonding of divalent cations with carboxyl groups on one pectin strand was found stronger than intermolecular bonding to neighboring pectin strands (with ring-oxygen atoms from hydroxyl groups).

Based on the above studies it can be concluded that carboxyl groups are responsible for metal ion binding, since esterification of pectin reduced metal binding capacity due to a decrease of carboxyl groups. The presence of carboxyl groups in pectin was also confirmed by FTIR studies by Synytsya et al. (2003). Thus carboxyl groups are one of the metal binding groups present in pectin and play an important role in metal binding.

The adsorption of metal ions by sugar beet pulp (agricultural waste) was studied by Reddad et al. (2002). Three intrinsic acidity constants K_{a1}^{int}, K_{a2}^{int}, and K_{a3}^{int} were determined by using potentiometric titration. Due to the heterogeneity of sorbent material, intrinsic acidity constants for each functional group were considered in the modeling. According to this model, three surface acidity constants (carboxyl and two

phenol moieties) were defined by mass action laws with an electrostatic correction term due to surface charge. The formation of inner–sphere complexes was assumed for the adsorption equilibrium.

For example in the case of carboxyl groups, the reactions are:

$$\equiv COOH + Me^{2+} \leftrightarrow \equiv COOMe^{+} + H^{+} \tag{2.1}$$

$$K^{Int}_{\equiv COOMe} \approx \frac{\{\equiv COOMe^{+}\}\{H^{+}\}}{\{\equiv COOH\}\{Me^{2+}\}} \exp\left(\frac{F\psi o}{RT}\right) \tag{2.2}$$

In above equation F is the Faraday constant and ψo is the zeta potential. The diffuse layer model was considered to determine the relationship between surface potential and surface charge.

Smith et al. (1999) discussed uncertainty involved in system definition and experimentation for speciation determination. In this article experimental uncertainty was explained for proton interactions with Suwannee River fulvic acid (SRFA). It was observed that the uncertainty associated with electrode calibration could be large and its contribution to overall total uncertainty was substantial. A Monte Carlo simulation approach showed the presence of large uncertainty at high pH (>9 - 10) and low pH (< 4).

Owing to uncertainty associated with classical solution schemes for modeling of sorption behavior of heterogeneous sorbents, the research work by Cernik et al. (1995) utilized the regularization method, which provides a stabilization of the resulting affinity distributions. The researchers showed that determination of affinity spectra could be

obtained by a constrained least-squares regularization technique. The employed regularization method introduced stabilization of the optimization problem which otherwise is an ill-posed problem because an equally good fit of data points can be obtained with different distributions.

Brassard et al. (1990) calculated binding site concentrations and corresponding pK_a values by using linear programming (LP) for a monoprotic model. On comparing results of the LP technique with experimental titration data, the researchers confirmed the flexibility of LP to resolve sites of low concentration. An objective function was constructed, which contained a set of linear equations and constraints (non-negativity of site concentration in this case) to limit the scope of the solution. The same method of forming an objective function was adopted by Smith and Ferris. (2001).

Smith and Ferris (2001) proposed a regularized least squares pK_a spectrum approach to determine proton stability constants. The resulting pK_a distributions obtained by a regularized least squares method (Cernik et al., 1995) for hydrous ferric oxide (HFO) were found to be consistent with theoretical binding site stability constants for crystalline iron oxides.

2.2 Dynamics studies with modeling

Antunes et al. (2003) conducted a basic investigation of copper removal by *Sargassum* sp. in a batch reactor. A shaking rate of 100 rpm was sufficient to achieve equilibrium

metal uptake in 30 min. Increase in pH for batch experiments increased the sorption of copper, but all the experiments were carried out at pH values lower than 6.0 to avoid insoluble copper hydroxide formation. A pseudo first-order Lagergren model and second-order model were used for kinetic modeling. The authors concluded that biosorption was the rate-limiting step because the sorption followed a pseudo second-order model. However, this conclusion may not be valid because a good model fit does not necessarily indicate the real nature of the rate limiting step. In many biosorption cases, diffusion rather than the chemical reaction was the rate limiting step.

In the studies by Cossich et al. (2002), the kinetics of chromium biosorption by inactive algal biomass were fast and reached 60% of the total sorption capacity in ten minutes. The sorption of chromium on brown algae reached its highest capacity at pH 4 and at 40°C. The alginate present in the brown algae was responsible for the metal uptake.

A first-order rate expression with respect to the binding sites was used by Ajmal et al. (2000) to describe the dynamics of adsorption of divalent cations by orange peels.

Though the Lagergren model may not reflect the true nature of sorption kinetics, it was employed to model dynamics in the current research due to its simplicity and good fit. Very few biosorption studies employ more complex mass transfer based models. An example of such a model is the work of Volesky (2003). It was found that for biosorption processes that are mainly based on ion exchange, uptake of metal ions into the biomass

should be accompanied by the release of protons (or other ions). The diffusion coefficient for protons is higher than that for heavy metal ions present in dilute aqueous solutions. The assumption that the overall sorption rate is controlled by heavy metal mass transfer is therefore sound. However, this level of modeling goes beyond the scope of this thesis, due to complexity associated with the model.

2.3 Comparison of biosorbent material and isotherm study

Ajmal et al. (2000) studied the ability of orange peels to remove divalent cations from aqueous solutions. Ni^{2+} was found to have a higher affinity to orange peels compared to other cations like Cu^{2+}, Pb^{2+}, Zn^{2+} and Cr^{2+}. It was observed that adsorption increased as the contact time and temperature increased. The highest metal uptake was reported at 2 hours of contact time for 50°C. An increase in temperature raised the equilibrium constant Kc, from which a decrease in Gibbs energy can be inferred, which in turn indicates that the adsorption process is endothermic. Regeneration studies in batch showed that 76% of the adsorbed Ni^{2+} could be removed with 0.05 M HCl.

Kartel et al. (1999) conducted experiments to understand and evaluate the adsorption of different heavy metals on industrially manufactured pectins. The studies showed a selectivity sequence $Pb^{2+} >> Cu^{2+} >> Co^{2+} >> Ni^{2+} >> Zn^{2+} >> Cd^{2+}$, wherein the lead ion had a higher affinity than other ions. The studies further revealed that Cd^{2+} and Zn^{2+} ions were poorly adsorbed on the pectin. In conclusion, the authors stated that while no generally recognized theory of heavy metal adsorption on pectin existed, the prominent

factor responsible for metal uptake could have been the formation metal pectate due to ion binding to the polymeric framework of pectin *via* hydroxyl groups of the polysaccharide matrix or carboxyl groups of galacturonic acid.

In a study by Pangnanelli et al. (2000), a culture of *Anthrobacter* sp. was used as biosorbent material to sorb copper, cadmium and iron ions. After determining two functional groups by potentiometric titration, the adsorption isotherm studies were carried out using a method called 'subsequent additions method' (SAM). This method was used to save biosorbent material as well as to improve control of the experimental conditions by decreasing variability of the sorbent between different points of the same isotherm.

Cohen-Shoel et al. (2002) investigated the adsorption capacity of the aquatic fern *Azolla filiculoides,* which contains approximately 8-10% (w/w) pectin in its cell wall. The metal ion (Sr^{2+}) found in radioactive waste was fed in the form of its nitrate solution to a glass column filled with dried *Azolla* biomass. The ions originally present, like Ca^{2+}, Mg^{2+}, Na^{+} and K^{+}, were released into eluate. Thus it was suggested that *Azolla* biomass has a higher affinity for Sr^{2+} compared to the originally present cations. The sorption capacity of *Azolla* (0.8 meq Sr^{2+}/g) was higher than that of sugar beet pulp (0.6 meq Sr^{2+}). The increase in effluent pH after *Azolla* biomass saturation with Sr^{2+} indicated the competition between protons and Sr^{2+} for the same binding sites. Prior to saturation, the effluent pH was lower due to a release of protons during Sr^{2+} binding.

An alkaline hydrolysis of sugar beet pectin to change the rheological properties of the polymer was carried out by Harel et al. (1998). The extracted sugar beet pectin was treated with calcium chloride solution to form gel particles of an average size of 3 mm. The cadmium binding capacity of sugar beet pectin gel beads was 4.6 (mg of Cd^{2+} / g of dry gel), which was higher than the binding capacity of alginate gel beads (4.1 mg of Cd^{2+}/g of dry gel).

Davis et al. (2003) described different polysaccharides present in algal cells. The structure of alginate was studied extensively to understand the significance of two important linear polysaccharides, mannuronic acid and guluronic acid, which are the components of alginate. The affinity of algae for heavy metals was related to a higher concentration of guluronic acid residues.

Grant et al. (1973) reported on three important factors affecting the binding of metals to pectin, which are

- Geometry of the ligands (i.e., the intermolecular stereochemistry).
- Separation between unit charges on the chain (i.e. polyelectrolyte effect).
- Cross association.

The authors proposed the egg-box model to explain the structure of the pectin molecule and the interaction of divalent cations with pectin chains.

According to Dronnet et al. (1997), the binding capacities for copper and lead cations were higher than those for other metal ions like cadmium and zinc in the case of processed sugar-beet pulp (SBP). The binding levels of Cu^{2+} and Pb^{2+} were observed to be higher than expected based on the cation exchange capacity. It was stated that the binding mechanisms governing the binding of SBP were more complex for Cu^{2+} and Pb^{2+} than for the weakly bound cations. Adsorption and/or chelation involving hydroxyl functions could have been an additional binding mechanism, along with electrostatic attraction for strongly bound cations like Cu^{2+} and Pb^{2+}.

Ca-alginate based ion-exchange resin was prepared by dispersing powdered sodium alginate in $CaCl_2$ solution (Chen & Wang 2001). A pH increase was observed as Ca-alginate resins remained in suspension for longer time. It was inferred that the Ca-alginate resins have ion exchange properties. Apparently protons from the solution were taken up in exchange for Ca by binding site (***R***), increasing the pH according to the following equations:

$$[H^+]_{decreased} = 2[Ca^{2+}]_{increased} \tag{2.3}$$

$$2H^+ + [Ca^{2+}\boldsymbol{R}] = Ca^{2+} + [H_2\boldsymbol{R}] \tag{2.4}$$

2.4 Biosorption equilibrium modeling

The most commonly used equilibrium models are the Langmuir (Equation 3.18) and the Freundlich (Equation 3.20) isotherms. Annadurai et al. (2003) primarily discussed the adsorption affinities for Cu^{2+}, Co^{2+}, Ni^{2+}, Zn^{2+} and Pb^{2+} on banana and orange peels and

found that an increase in pH increased metal adsorption. Scanning electron microscope (SEM) images, and energy dispersion system (EDS) spectra and Zeta potential studies, corroborated the existence of Cu and Zn metals on the peel surface. The modeling of the experimental data showed that the Freundlich isotherm describes the sorption isotherms better than the Langmuir isotherm.

Agricultural wastes like *Citrus sinesis* (grapefruit) skin and coffee husk were treated with different divalent metal ions like Hg^{2+}, Pb^{2+} and Zn^{2+}. The Freundlich adsorption isotherm was used to fit the experimental data. The experimental data were in good agreement with the Freundlich model (Jumle et al., 2002).

A novel approach for modeling heavy metal biosorption was adopted by Schiewer and Volesky (1995). The authors chiefly considered the exchange of ions for protons present on biosorbent surface groups like carboxyl and sulfate. The model considered the reaction between divalent metal ions and deprontonated acidic groups (in this case carboxyl and sulfate). One-site and two-site sorption models were used to fit the sorption data and corresponding parameters were calculated by nonlinear regression. The complexity of the two-site model was decreased by using the already determined site concentration and pK_a from titration data. This model approach was found to be more flexible than traditional isotherm models because, using the same parameters, the model could be fitted for data obtained at different pH values, since it considers the effect of pH on metal uptake.

Volesky (2003) highlighted seven different equilibrium simulation models. He described surface complexation models (SCM) which are based on surface charge generated from amphoteric surface sites. The most common SCM model is the two-pK_a triple-layer (TL) model which assumes that an electrical double layer consists of three parts divided by the surface plane (o-plane), the outer Helmholtz plane (d-plane), where the diffusive double layer starts, and the inner Helmholtz plane (β-plane), where ions form complexes with surface groups. Though this model is more accurate than other models like the Langmuir model, its complexity makes it less desirable in the current research.

Since the Langmuir and Freundlich models are simple and often able to fit sorption isotherms, they are widely used. However, the limitation of these basic models is that they do not have predictive power. For changing conditions (pH, ionic strength, competing metals, temperature) new model parameters have to be determined. While surface complexation models may be able to predict the effect of changing conditions, they are complex and not easy to use. In the present work, the Langmuir model and a modified pH-sensitive isotherm model are used, due to their comparative simplicity. Since ionic strength effects were not studied within this work, it was not necessary to utilize surface complexation models; this may be done in future work.

Chapter 3

Materials and Methodology

3.1 Biomass preparation, protonation and characterization

3.1.1 Biomass preparation

Pectin rich fruit materials like lemon peels, orange peels, grapefruit peels, apple residues (peels, kernel and pomace) and grape skins were selected because of their high pectin content and easy availability. Large quantities of all these materials are generated as waste materials by the fruit industries. These fruit materials were washed three times with nano-pure water (approximately 18 ohms resistance) to remove extraneous materials attached to the sorbent surfaces. Since the sorbents differed in their initial water content, the fruit materials needed to be dried until they reached a constant weight. This was accomplished by drying at 38-40^{o}C in the convection oven for 12 hours. The dried material was then ground and screened to obtain different particle sizes. The fruit materials were weighed before and after drying.

3.1.2 Protonation of lemon fruit waste

Performance of the biosorbent depends on the ionic state of the biomass and thus, like the synthetic resins, biosorbents can be prepared in different ionic forms such as protonated (H^+ forms). So called pectin peels, which are comprised of processed skins, seeds and peels (which will be referred as 'lemon fruit waste' and can be seen in Figure 3.1) was obtained from a citrus–juice processing company (Sunkist®). Pectin peels are produced

from juice manufacturing residues by leaching of the soluble sugars, followed by drying (Vincent 2001). This lemon fruit waste is commercially used for pectin extraction. According to the manufacturer (Sunkist®) the moisture content was approximately 10% and the pectin content was slightly greater than 28%.

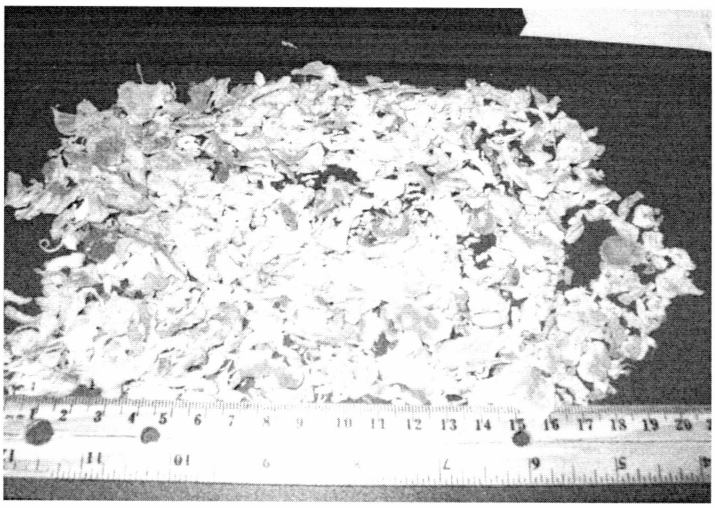

Figure 3.1: The preprocessed dried lemon fruit waste donated by Sunkist®

The fruit materials were washed three times as described in section 3.1.1, followed by treatment with 0.1 N HNO_3 for six hours and 12 hours of drying at 38-40°C. Then the acid treated lemon waste was washed three times with nano-pure water to remove excess acid and hard ions like Ca^{2+}, and K^{+}, which are also called Group I metal ions by Buffle (1990). In the final stage these materials were dried, ground and sieved to obtain different particle sizes. The treatment with mineral acid is called protonation (Yang et al., 1999) which enhances the biosorption capacity of the biosorbent material by decreasing the competition of ions like K^{+}, and Ca^{2+} with heavy metal ions like Cd^{2+}.

3.1.3 Characterization (using potentiometric titration)

Many complexation reactions occur among metals, ligands, and surfaces in the aquatic environment. Acid-base titrations are often used and have proven to be an excellent tool to investigate the chemical nature and concentration of reactive sites on heterogeneous sorbent surfaces in many adsorption studies. The weighed protonated lemon waste (0.503g) of size 0.7-0.9 mm (diameter) was hydrated with 50 mL of nano-pure water for two hours to obtain a biosorbent concentration of 10.06 g/L, with continuous nitrogen bubbling to avoid formation of carbonic acid. The higher concentration of biosorbent was chosen to ensure acid-base reactions could be easily observed. A volume of 0.05 mL of 0.071 N NaOH was added to the reaction flask ,agitated with magnetic stir bar at 120 rpm after three minutes of equilibration and the corresponding changes in pH were noted. The base addition was repeated until pH reached 11.05. The time required to obtain a constant pH was increased from 3 min to 7 min at higher pH values (pH $\geq$ 6). The same procedure was repeated for a blank titration of 50 mL nano-pure water on the same day. From the experimental data the surface charge was calculated as described below (Equation 3.1).

In biosorption chemical modeling development, it is essential to have a basic characterization of the sorbent material. The presence of different binding groups and their concentration were determined with the help of modeling techniques (Pagnanelli et al., 2000, Smith and Ferris 2001, and Yun et al., 2001). The change in surface charge concentration (charge excess) with pH can be obtained by resolution of titration curves

into concentration-pK_a spectra. The titration profile can be obtained by discrete and continuous affinity distribution techniques (Cerink et al., 1995)

3.1.4 Titration data processing technique

The predications of charge excess on the biosorbent surface after each titrant addition and determination of acidity constants are solutions of a nonlinear equation (Equation 3.5). The classical least-square methods have often been employed to determine the acidity constants for a given number of discrete sites, but the solution of minimizing any nonlinear equation with a discrete model is dependent on the number of binding sites (acidity) constants as well as on initial parameter guesses and difficulties in attaining convergence (Cernik et al., 1995). To circumvent the associated difficulties, a fully optimized continuous (FOCUS) pK_a spectrum technique has been developed by Smith and Ferris (2001) to fit acid-base titration data and to evaluate binding site acidity constants through additional non–negativity constraints and regularizing functions. This technique is advantageous because it optimizes for both the smoothness of the continuous pK_a spectrum and for the goodness of fit, simultaneously, to determine the full extent of surface chemical heterogeneity. The determination of pK_a values is always a crucial and important factor for modeling of isotherms. While it is easier to derive a discrete model with a limited number of acidic sites, the continuous spectrum technique is chosen in this work because it not only gives a stable solution, but also models binding site concentrations with corresponding pK_a and, thus, it does not require predetermination of the binding sites.

The FOCUS technique, which neglects electrostatic effects and site-site interactions, provides an apparent spectrum which may not be representative of the true affinity spectrum. However, since other current techniques can not give a true affinity spectrum either, an apparent spectrum obtained from the FOCUS technique will be the best compromise. The following steps are performed in this technique:

The excess charge after the i^{th} addition of titrant is expressed as:

$$b_{measured,i} = \frac{C_{bi} - C_{ai} \pm [H^+]_i - [OH^-]_i}{B} \tag{3.1}$$

Where, $b_{measured,i}$ is the charge excess (mol/g) which is calculated from experimental data, C_{bi} and C_{ai} are the concentrations (mol/L) of base and acid added respectively, $[H^+]_i$ and $[OH^-]_i$ are the proton and hydroxyl concentrations (mol/L), respectively, in the solution, and B is the biosorbent concentration (g/L).

Many different sets of acid-base reactions could be occurring but a monoprotic model is considered for the current research because of its simplicity. Corresponding b_i are calculated as a function of the speciation parameters, which are the number of different acidic sites (m), and total concentration of each weak acid site ($L_{T\,j}$, mol/L) having an acidity constant $K_{CH\,j}$ and a constant offset term So. The total concentration (L_T) for any binding site consists of the concentrations of free binding site (L^-) in mol/L and the protonated binding site (HL). The charge excess (Equation 3.5) can be calculated by combining Equations 3.3, and 3.4 for all j sites.

$$[H^+] + [L^-] \leftrightarrow [HL] \tag{3.2}$$

$$K_{CH} = [H^+]\,[L^-] / [HL] \tag{3.3}$$

$$[L_T] = [L^-] + [HL] \tag{3.4}$$

$$b_{cal,i} = \sum_{j=1}^{m} \left(\frac{L_{T\,j} K_{CH\,j}}{K_{CH\,j} + [H^+]_i} \right) + So \tag{3.5}$$

The offset term *So* is added in order to account for the positive charges on the surface since a monoprotic model only accounts for the negative surface charges while many natural poly-electrolytes are positively charged. According to Brassard et al. (1990) for monoprotic models the offset term is the acid neutralizing capacity (ANC).

In fitting of the monoprotic model (Equation 3.5) to experimental data of the charge excess ($b_{measured,i}$) calculated by Equation 3.1, the model parameters cannot be fitted independently. Stability constants and site concentrations are interdependent, which poses problems in model fitting because there is no unique solution. The pK_a spectrum approach involves fixing a sequence of closely spaced pK_a values (2, 2.2,...,11, 11.2) and randomly assigning initial ligand concentrations for each pK_a. The model (Equation 3.5) is transformed into a more simple form as given in Equation 3.6.

$$A \times X = b_{cal,i} \tag{3.6}$$

$$A(i,j) = \frac{K_{CH\,j}}{K_{CH\,j} + [H^+]_i} \quad \text{for } i = 1\ldots n \text{ and } j = 1\ldots m \tag{3.7}$$

Where, A is an n x (m+1) matrix which represents the degree of dissociation, X is a (m+1) x 1 vector of unknown total site concentrations (L_T) and b is an n x 1 vector of charge excess (n- total number of titration data points, m-total number of binding sites).

Equation 3.6 can be solved in many different ways, but finding unique solution to it is a cumbersome process (Smith et al. 2001). The linear Equation 3.6 was solved by using Matlab®–Optimization toolbox (The Math Works Inc.). Due to the absence of any unique solution, Equation 3.6 is considered as an ill-posed problem.

Cernik et al. (1995) approached this ill-posed problem by regularization. Regularization was carried out by imposing some constraints before solving Equation 3.6 with *a priori* information about the system. In this case, the non-negativity of site concentration was the imposed constraint on the system. Thus, the outcome of could be regularized for smoothness by minimizing the following function which is called regularized least-squares optimization.

$$\text{Minimize } SS + \lambda R \tag{3.8}$$

$$SS = \sum_{i=1}^{m} (b_{cal,i} - b_{measured,i})^2 \quad \text{and} \quad X \geq 0 \tag{3.9}$$

$$R(X_1,.....X_m) = \sum_{j=2}^{m-1} (X_{j-1} + 2X_j + X_{j+1})^2 \tag{3.10}$$

The *SS* term is the sum of square terms for nonlinear regression without regularization and *R* is the sum of squares of finite difference approximation of the second derivatives which is called regularizing function and it increases smoothness of solutions. According to Cernik et al. (1995), *R* is small for affinity distributions which have small mean curvature, and is large for strongly oscillating functions. Thus, there are two terms to be optimized (*SS* and *R*) and the optimal solution depends on the regularization strength

parameter (λ). Equation 3.8 is minimized by changing the values of the regularization strength parameter (starting value of $\lambda = 0$). The simple form of (3.8) is given by:

$$\text{Minimize } (SS \pm \lambda R) = [Minimize(SS - SS_k)^2 + (0 - \lambda_k R_k)^2]^{0.5} \quad (3.11)$$

The value of λ is varied for a total of k different values and k^{th} values of sum squares (SS_k) and regularization R_k are determined.

3.2 Dynamics studies with modeling

3.2.1 Dynamics studies

Batch kinetic experiments were carried out to determine the time required to reach the equilibrium for lemon fruit waste of size 0.177 mm. A biosorbent sample (0.2g) was mixed with 100 mL of metal (Cd) bearing solution of an initial concentration of 141 ppm (2.50 meq/L) in 200 mL Erlenmeyer polyethylene flasks on a magnetic stirrer at 120 rpm. A 10 mL sample of treated solution was taken out and filtered at different time intervals ranging from 5 min to 60 min. The solution in the flask was at a constant pH of 3 or 5, which was maintained by adding 0.1 N HNO_3 or NaOH. The concentration of heavy metals in the initial solution and in the final solution was determined by AAS (Perkin-Elmer AAnalyst 300) having an air-acetylene burner and controlled by an IBM personal computer.

To evaluate the effect of biosorbent particle size on dynamics of biosorption, reactions were carried out by using 0.2 g of three different particle sizes (diameters = 0.240 mm,

0.420 mm, and 0.710 mm). The sorbent material was contacted with 0.2 liter of 0.8 meq cadmium ion solution (cadmium nitrate). The same procedure, as above, was repeated at pH 5 and the modeling studies were performed as described in the following sections.

3.2.2 Kinetic modeling

The kinetics of the metal binding were studied for two different initial concentrations in the separate studies (2.50 meq/L for pH studies and 0.8 meq/L for particle size studies) as mentioned in the previous section. The rate of any chemical reaction (except zero-order) depends also on the concentration of reactants. This aspect was not addressed in this study but should be fully investigated in future studies to learn in detail the effect of varying concentrations of metal ions.

For this research, two different kinetic models were used to model the experimental data of Cd^{2+} biosorption on lemon fruit waste at different pH values. The pseudo first-order Lagergren model is expressed as:

$$\frac{dq}{dt} = k_{1,ads}(qe - q) \tag{3.12}$$

Where qe (meq/g) and q are the amounts of adsorbed metal ions on the biosorbent at the equilibrium and at any time t, respectively; and $k_{1,ads}$ is the Lagergren rate constant of the first-order biosorption (min^{-1}). The model is based on the assumption that the rate is

proportional to the number of free sites. Integrating Equation 3.9 between the limits, $t = 0$ to $t = t$ and $q = 0$ to $q = q$ yields:

$$\int_0^q \frac{dq}{(qe - q)} = k_{1,ads} \int_o^t dt$$

$$\log (qe - q) = \log qe - \frac{k_{1,ads} t}{2.303} \tag{3.13}$$

Linear plots of *log* (*qe-q*) versus *t* were plotted to indicate the applicability of this kinetic model and to determine rate constant and *qe* from the slope and intercept, respectively.

The pseudo second-order model is based on the assumption that biosorption follows a second-order mechanism, whereby the rate of sorption is proportional to the square of the number of unoccupied sites:

$$\frac{dq}{dt} = k_{2,ads} (qe - q)^2 \tag{3.14}$$

Where $k_{2,ads}$ is the rate constant of second-order biosorption (g/meq-min). Integrating Equation 3.14 for the boundary conditions $t = 0$ to $t = t$ and $q = 0$ to $q = q$ and linearization yields:

$$\frac{t}{q} = \frac{1}{k_{2,ads} qe^2} + \frac{t}{qe} \tag{3.15}$$

The parameters *qe* and $k_{2,ads}$ are calculated from the slope and the intercept of the plot *t/q* versus *t*. It is important to notice that it is not necessary to estimate the experimental value of *qe* for the application of such a model.

3.3 Comparison of biosorbent materials and isotherm studies

3.3.1 Comparison of biosorption capacities

Before carrying out in-depth studies for isotherms, a comparison of metal uptake capacities and stability of several biosorbent materials was performed. The comparison between two or more sorbent materials can be considered fair if the same conditions (like pH, temperature) are maintained for all sorbent materials. Metal uptake capacities of the seven selected biosorbent fruit materials (lemon peels, orange peels, grapefruit peels, apple core, apple peels, apple kernel and grape skins) were determined by treating 0.1g of 0.7-0.9 mm pectin-rich fruit materials with a synthetic solution of $CdCl_2$ (containing 692.82 mg/L of Cd^{2+}) at pH 5. The solution was shaken for 6 hours with continuous maintenance of pH 5 by adding 0.1N NaOH or HCl. The selection of pH was based (Annadurai et al., 2003) on the fact that there is a lesser competition between Cd^{2+} ions and protons at this pH which leads to higher metal uptake compared to at lower pH values. The suspension of metal solution and biosorbent material was filtered and the concentration of metal in the liquid phase was determined by AAS. To distinguish between possible metal precipitation and actual metal sorption, controls were used

without biosorbent materials. The metal uptake per gram of biosorbent material was determined by employing the mass balance. If *Co* and *Ce* are the initial and final metal concentration (meq/L) respectively, *V* is the suspension volume (L) and *W* is the mass of biosorbent material (g), the equilibrium metal uptake *qe* (meq/g) can be calculated as:

$$qe = \frac{V(Co - Ce)}{W} \tag{3.16}$$

3.3.2 Isotherm experiments

Since sorption is affected by temperature, maintaining constant temperature during the sorption process is a basic requirement. Sorption isotherms are plots of the sorption uptake (*qe*) versus the final equilibrium concentration of the residual sorbate remaining in the solution (*Ce*) and the corresponding metal uptake can be calculated as given in Equation 3.16.

Based on the metal uptake capacity and the stability of the material, citrus peels were selected for further studies. The concentration of metal solution was varied in the range of 10-700 mg/L and treated with 0.1g of 0.7-0.9 mm biosorbent material at constant pH (3 or 5) as described above. Blank tests were also performed without biosorbent to investigate the removal which might occur via metal precipitation and adsorption on the pH electrode as well as the glass walls of flasks. The isotherm was plotted for varying final concentration of Cd^{2+} ion in the solution and equilibrium metal uptake.

3.3.3 SAM

For further equilibrium studies, a more reliable and less labor consuming experimental procedure called SAM (Pagnanelli et al., 2000) was used rather than performing individual experiments for each data point of the isotherm. This new procedure not only decreased variations from point to point of an isotherm due to biomass heterogeneity, but also pH was easily controlled using this method. The procedure is explained as follows:

1) An amount of 0.1 g of the citrus peels was contacted with 50 ml nano-pure water for the required equilibration time (60 min), which had been determined in preliminary kinetic experiments as discussed in section 3.2. Then a small volume of concentrated metal solution of known concentration (0.05 mL initially) was added to the suspension. The suspension was constantly agitated by using a magnetic stir bar until equilibrium was reached (1 hour). The pH was controlled by adding 0.01/0.1 N NaOH.

2) At equilibrium a small volume of suspension u = 1.5 mL was taken out and filtered using Whatman 40 ashless filter paper and the metal concentration in the filtrate was analyzed by AAS.

3) The next addition of the concentrated metal solution was made and the above steps were repeated. The increase in solution volume due to these additions was taken into account in calculating the equilibrium uptake after each step using Equation 3.17. The

equilibrium metal uptake (meq/g of biosorbent) by the biosorbent was calculated from the mass balance, considering the amount of metal added and removed in all prior steps. Repeated additions of concentrate were made after the system reached the equilibrium. Cc (meq/L) was the concentration of metal solution added of volume v_i (L), C_i was the equilibrium metal concentration after step i, V and u (L) were the total suspension volume and drawing volume, respectively and B_i was the biosorbent concentration in (g/L).

$$v_i \times Cc + q_{i-1} \times B_{i-1} \times (V_{i-1} - u) + (V_{i-1} - u) \times C_{i-1} = C_i \times V_i + q_i \times B_i \times V_i \qquad (3.17)$$

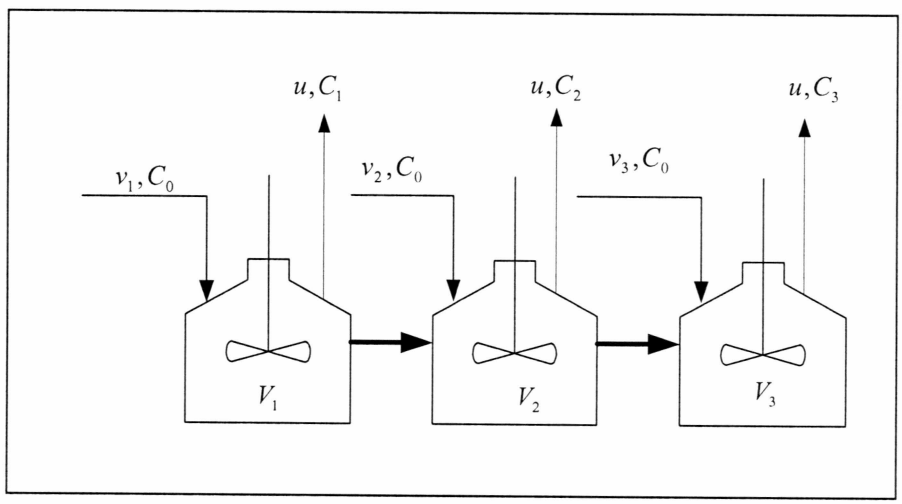

Figure 3.2: The subsequent additions method (Pagnanelli et al., 2000)

3.4 Biosorption equilibrium modeling

Modeling the equilibrium isotherm data is important for the industrial application of biosorption since it gives information for comparison among different biomaterials under different operational conditions, and facilitates designing and optimizing operating

procedures. To examine the relationship between equilibrium metal uptake (*qe*) and final concentrations (*Ce*) at equilibrium, sorption isotherm models are employed for fitting the data, of which the Langmuir and Freundlich equations are the most widely used. The Langmuir isotherm relationship is given as:

$$qe = \frac{\theta \; q_{max} \; Ce}{(1 + \theta \; Ce)} \tag{3.18}$$

Where θ (L/meq) is the equilibrium adsorption constant which is related to the affinity of the binding sites and q_{max} (meq/L) is the maximum amount of metal ion per unit mass of biosorbent to form a complete monolayer on the surface.

The Langmuir parameters can be determined from a linearized form of Equation 3.18 (by plotting *Ce/qe* vs. *Ce*), represented by:

$$\frac{Ce}{qe} = \frac{1}{\theta \, q_{max}} + \frac{Ce}{q_{max}} \tag{3.19}$$

The Freundlich equation is given by:

$$qe = k_f Ce^{1/\eta} \tag{3.20}$$

Where k_f and η are the Freundlich constants and are related to the adsorption capacity of the biosorbent and the adsorption intensity. To simplify the determination of k_f and $1/\eta$, Equation 3.20 can be linearized in logarithmic form and unknown parameters are determined by plotting log *qe* vs. log *Ce*.

$$\log qe = \log k_f + \frac{1}{\eta} \log Ce \qquad (3.21)$$

The choice between Langmuir and Freundlich isotherms depends mainly on the nature of equilibrium data. In many equilibrium studies the metal uptake data attain a plateau which corresponds to the Langmuir model (q_{max}). Though both the isotherms consider the presence of free sites rather than ion exchange, these isotherm models are widely used for modeling equilibrium data because of their simplicity.

In the ion exchange modeling approach, it is assumed that other ions are replaced by metal ions. However, ion exchange constants do not account for the change in cation exchange capacity with pH because of protonation-deprotonation of weakly acidic sites (for cation exchange). Therefore, the use of ion exchange constants at varying pH values does not reflect the true nature of the reactions in the system. At constant pH values modeling with ion exchange constants can yield the same behavior as a Langmuir isotherm, since the ratio of proton-occupied and free sites is constant at constant pH. Due to its simplicity and good representation of the experimental data, the Langmuir isotherm (referred to as Langmuir model in plots) is predominantly used for this study.

Additionally, a model based on a more realistic combination of ion exchange and acid/base reactions developed by Schiewer and Volesky (1995) was used for modeling experimental data obtained using the SAM technique for protonated lemon waste. For this sorbent material, acid/base properties were determined, and were used as input for the model.

The pH-sensitive model proposed by Schiewer et al. (1995) is very useful to reflect that biosorption is a process involving ion exchange between metal ions and protons as well as binding to already unprotonated sites. In the case of the Langmuir model only unprotonated free sites act as binding sites, neglecting exchange with other ions. This is only a reasonable assumption at higher metal concentration, where binding of the displaced ion is very low. The pH-sensitive model considers that binding of the displaced ion (proton) is a reversible reaction even at a lower concentration of metal ions, which is a realistic scenario. A major advantage of the model is that the effect of pH on metal binding can actually be predicted using the same metal binding constants for different pH values. The model for the pH-sensitive isotherm equation is derived by using the following equations.

If $[M^{2+}]$ is the concentration of divalent metal ion which forms a complex compound with an acidic site with concentration $[L^-]$, then the metal binding constant is given as K_{LM}.

$$[M^{2+}] + 2\,[L^-] \leftrightarrow 2\,[LM_{0.5}] \tag{3.22}$$

$$K_{LM} = [LM_{0.5}]^2 \left(\frac{W}{V}\right)^2 / [M^{2+}]\,[L^-]^2 \quad \text{(L/mmol)} \tag{3.23}$$

$$[L_T] = [L^-] + [HL] + [LM_{0.5}] \quad \text{(mmol/g)} \tag{3.24}$$

The mass balance for total metal ions is given by

$$[M_T] = [M^{2+}] + 0.5\,[LM_{0.5}] \left(\frac{W}{V}\right) \quad \text{(mmol/L)} \tag{3.25}$$

By reformulating above equations one can derive

$$q_M = 0.5[LM_{0.5}] = \frac{0.5[L_T](K_{LM}[M^{2+}])^{0.5}}{(1 + K_{CH}[H^+] + (K_{LM}[M^{2+}])^{0.5}} \quad \text{(mmol/g)} \quad (3.26)$$

The above Equation 3.26 was used to fit the data obtained by the subsequent additions method for pH 3 and pH 5.

3.5 Average of sum of squared errors

The average of the sum of squared errors (*SSE/p*) was calculated for every model fit by taking the square of the difference between values of metal uptake, obtained from experimental data (*q*), and those of determined by a model (*qm*), and dividing it by the number of data points (*p*) for each data set.

$$SSE/p = \frac{\sum_{1}^{p}(q - qm)^2}{p} \quad (3.27)$$

Chapter 4

Results and Discussion

4.1 Comparison of biosorbent materials

Figure 4.1 shows the metal uptake capacities of pectin-rich biosorbent materials. It can be observed that grape skins have the highest metal uptake capacity of 1.20 meq/L, followed by orange peels, apple core and lemon peels. The stability of these materials was a crucial factor in the selection of pectin-rich fruit materials for future isotherm studies. The apple fruit waste and grape skin started disintegrating at pH 5 after 2 hours of contact with a cadmium solution with an initial concentration of 692.82 mg/L. The citrus peels (lemon, orange and grapefruit peels) were selected for further studies because of their higher mechanical strength compared to apple residues and grape skins along with good metal uptake properties, supporting the first hypothesis.

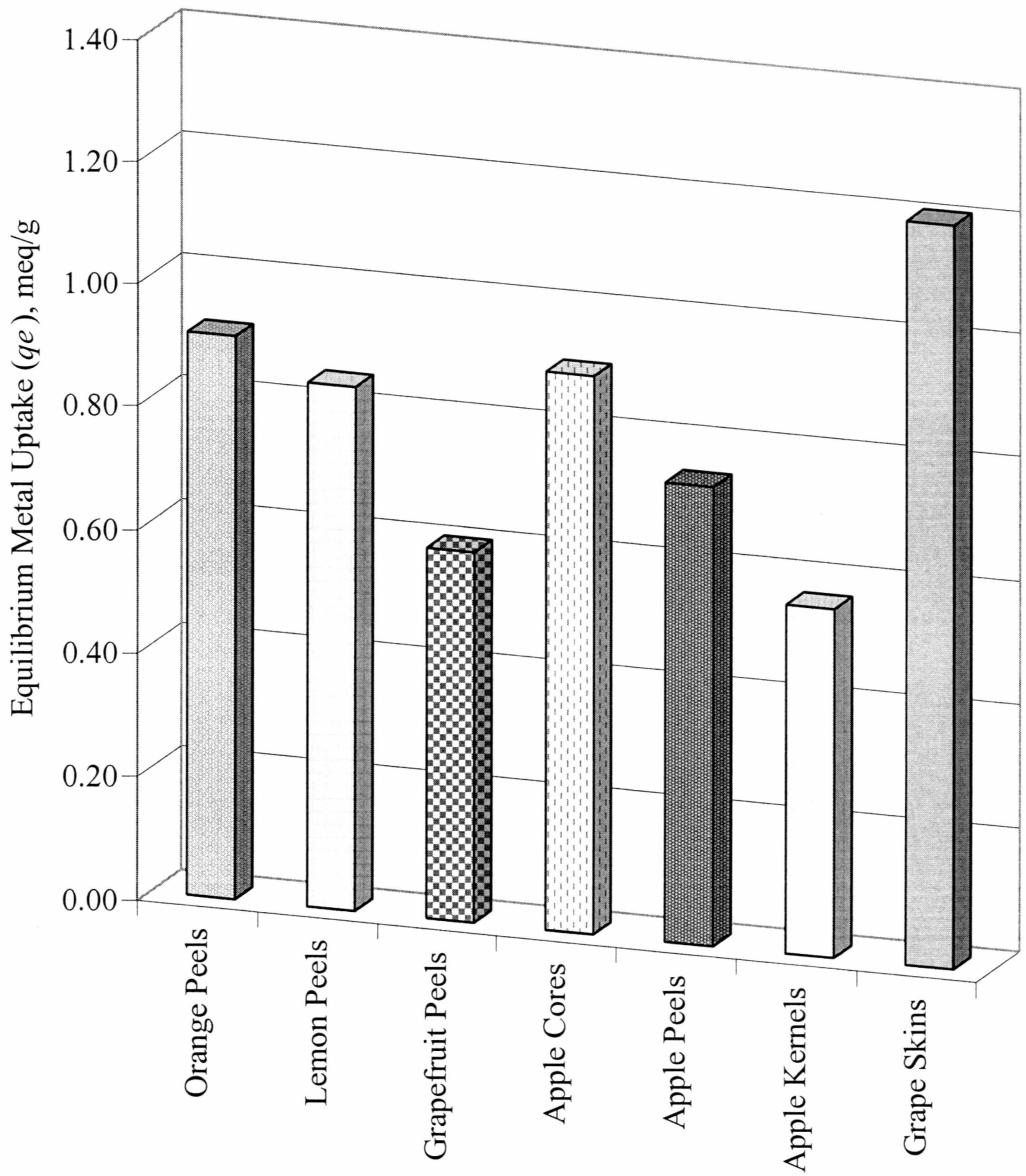

Figure 4.1: Comparison of metal uptake capacities of petin-rich fruit materials

4.2 Potentiometric titration

After transforming titration data according to Equation 3.1, the charge excess (b_i) versus pH was plotted as shown in Figure 4.2 (symbols). The presence of inflections around pH 4 and 8.5 was evident and could provide a first indication of binding sites on the biosorbent material. Previous studies (Lee et al., 1999) have already proven the presence of carboxyl groups in pectin. Carboxyl groups typically have pK_a values between 3 and 5 (Buffle, 1990). It is reasonable to infer that the carboxyl group is one of the prominent groups present on the lemon fruit waste material and that it is responsible for the inflection at pH around 4.

A more sophisticated analysis of the pK_a values was performed through minimizing the function $SS + \lambda R$ (Equation 3.8) using the FOCUS technique with regularization (Smith et al., 2001). Applying the algorithm in Matlab® (codes in Appendix) resulted in the continuous pK_a spectrum represented in Figure 4.3. The ordinate represents the site concentration (L_T) in mol/g while the abscissa is the pK_a range. The area under each peak is the total site concentration having a particular pK_a, which corresponds to the highest point of each peak. The total site concentrations and pK_a values are tabulated in Table 4.1. The overall (summation of the concentration of all the sites) site concentration is found to be 1.6 mmol/L. The two main sites, with quantities of 0.82 and 0.52 mmol/g (together 84 % of the total sites), had pK_a values of 3.8 and 8.4, respectively. Buffle (1990) reported pK_a values in the range of 2.6-4.7 for carboxyl groups found in organic compounds. The detection of $pK_{a1} = 3.8$ in the pK_a spectrum could be attributed to the

presence of carboxyl groups in lemon fruit waste. FTIR studies by Lee et al. (1999) have already confirmed the presence of carboxyl groups in pectin, which is a substantial component of citrus fruit materials. These results support the second hypothesis that the carboxyl group is the dominant functional group in citrus peels. According to studies by Lee at al. (1999) and Reddad et al. (2002), the phenolic functional groups or moieties could correspond to pK_{a2}, and pK_{a3}.

The pK_a spectrum is further confirmed by comparing the charge excess obtained from FOCUS modeling with experimental values. Figure 4.2 shows the modeled charge excess curve (line) plotted along with the experimental data (symbols). The slight deviation of the modeled curve from experimental curve at higher pH values can be ignored because of high uncertainty (Smith et al., 1999) associated with pH measurement at higher pH values (9-10).

Table 4.1: Site concentrations with corresponding pK_a values using the pK_a spectrum

Site	Total site concentration mmol/g	pK_a
Site 1	0.82	3.8
Site 2	0.09	6.4
Site 3	0.52	8.4
Site 4	0.18	10.7

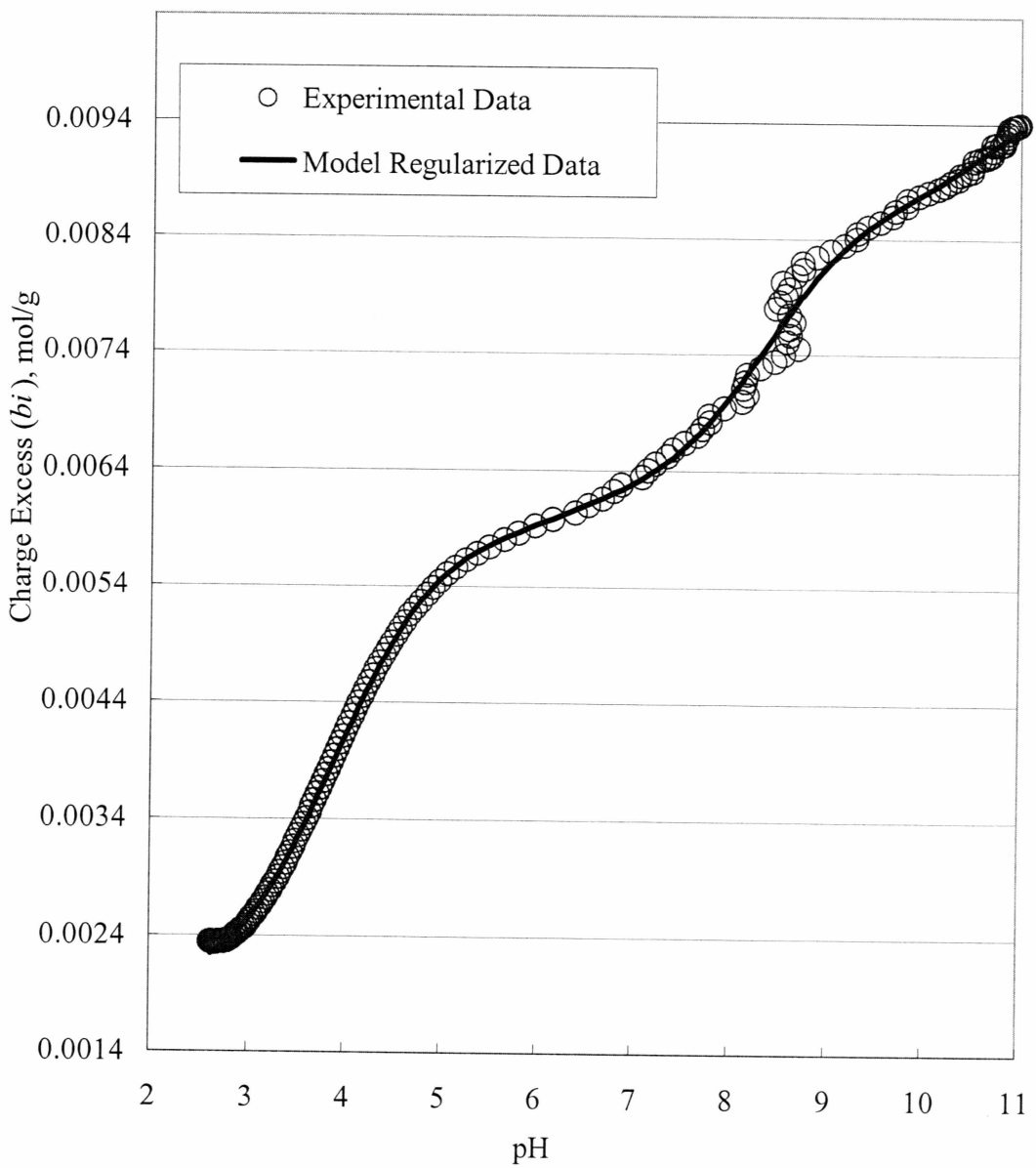

Figure 4.2: Comparison between charge excess curves obtained from experimental data points and a regularization model

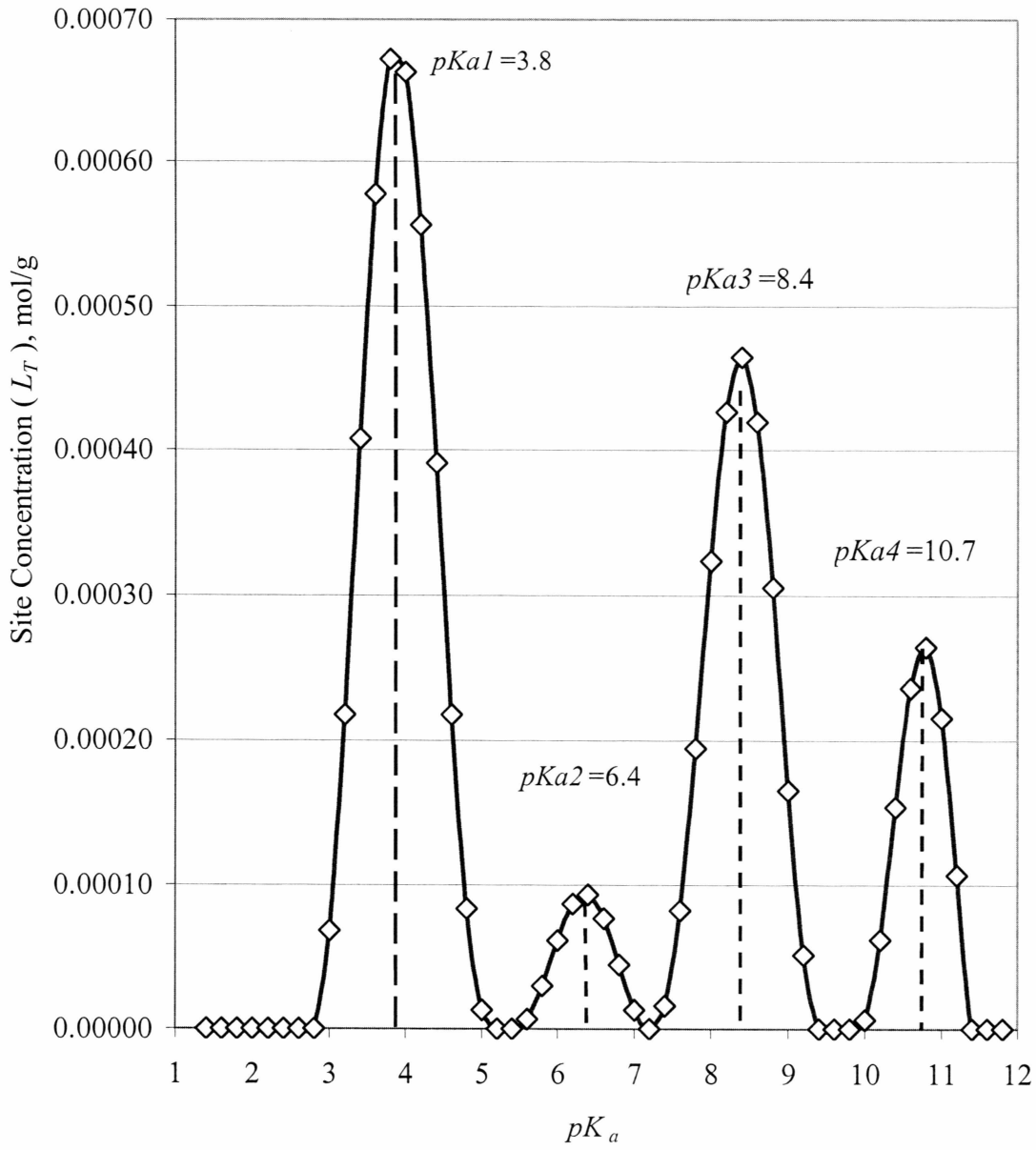

Figure 4.3: The regularized pK_a spectrum plotted after imposing the non-negativity of site concentration constraint

4.3 Kinetics

4.3.1 Influence of pH

Figure 4.6, in which the metal uptake (q) is plotted versus time (t), shows that the equilibration time at pH 3 and 5 was around 20 min. Nevertheless, all isotherm studies using this particle size of (diameter = 0.177 mm) should be carried out for 60 min to ensure attainment of equilibrium.

Figure 4.4 is a linearized plot for the first-order Lagergren model, according to equation 3.13. The Lagergren first-order rate constant ($k_{1,ads}$) and qe were determined from the slope and y-intercept of this plot, respectively. These values are listed in Table 4.2. The first-order model failed to estimate qe since the experimental values of qe (0.99 meq/L) were much higher than the fitted value (0.32 meq/L) for pH 5. This underestimation of the amount of binding sites is probably due to the fact that qe was determined from the y-intercept, which is most strongly affected by the metal uptake during the initial time intervals, which are not necessarily close to the equilibrium uptake. This appears to be a general disadvantage of using the linearized first order model. For pH 5, the first-order model was again plotted in Figure 4.4 using the experimentally determined qe as the y-axis intercept (log q_e) to calculate the corresponding first-order rate constant (in Table 4.2 as *Modified*). The resulting model predictions are shown in Figure 4.6.

The second-order plot of t/q against t (Figure 4.5) according to the linearized second order equation 3.15 resulted in straight lines with square of coefficient of correlation (R^2)

of 0.99 for pH 3 and 5 and led to the determination of the second-order rate constants ($k_{2,ads}$) and qe from the slope and the y-intercept. These values, which are listed in Table 4.2, were very close to the experimentally determined values of qe. The R^2 values for the second-order kinetic model were equal to 0.99 for either pH values while those for the first-order kinetic model were 0.83 and 0.95 for pH 5 and 3, respectively (Table 4.2). The pseudo second-order kinetics provided the best fit for the kinetic data. Using model equations, the corresponding metal uptake at different time intervals was back calculated and plotted in Figure 4.6. As it can be seen, the second-order model provides a good fit for either pH value, while the first-order model for pH 5 does not represent the experimental data. The modified first-order model (with log qe as y-intercept) provides an acceptable fit of the experimental data at larger time intervals (after 20 min), but has the lowest R^2 value of 0.61.

The better fit of the second order model is compatible with a 1:2 binding stoichiometry, where one divalent metal binds to two mono-valent binding sites. Therefore the second order model is plausible from a mechanistic standpoint.

A reason for first-order model discrepancies at pH 5 compared to pH 3 lies in the fact that at pH 3 the final concentration was still close to the initial concentration, whereas at pH 5 the metal concentration was reduced strongly (Figure 4.6). The kinetic model used here does not account for changes in the metal concentration. This factor should be included in future improvements in the kinetic modeling; experiments should be conducted at a range

of different concentrations to determine the reaction order with respect to the metal concentration.

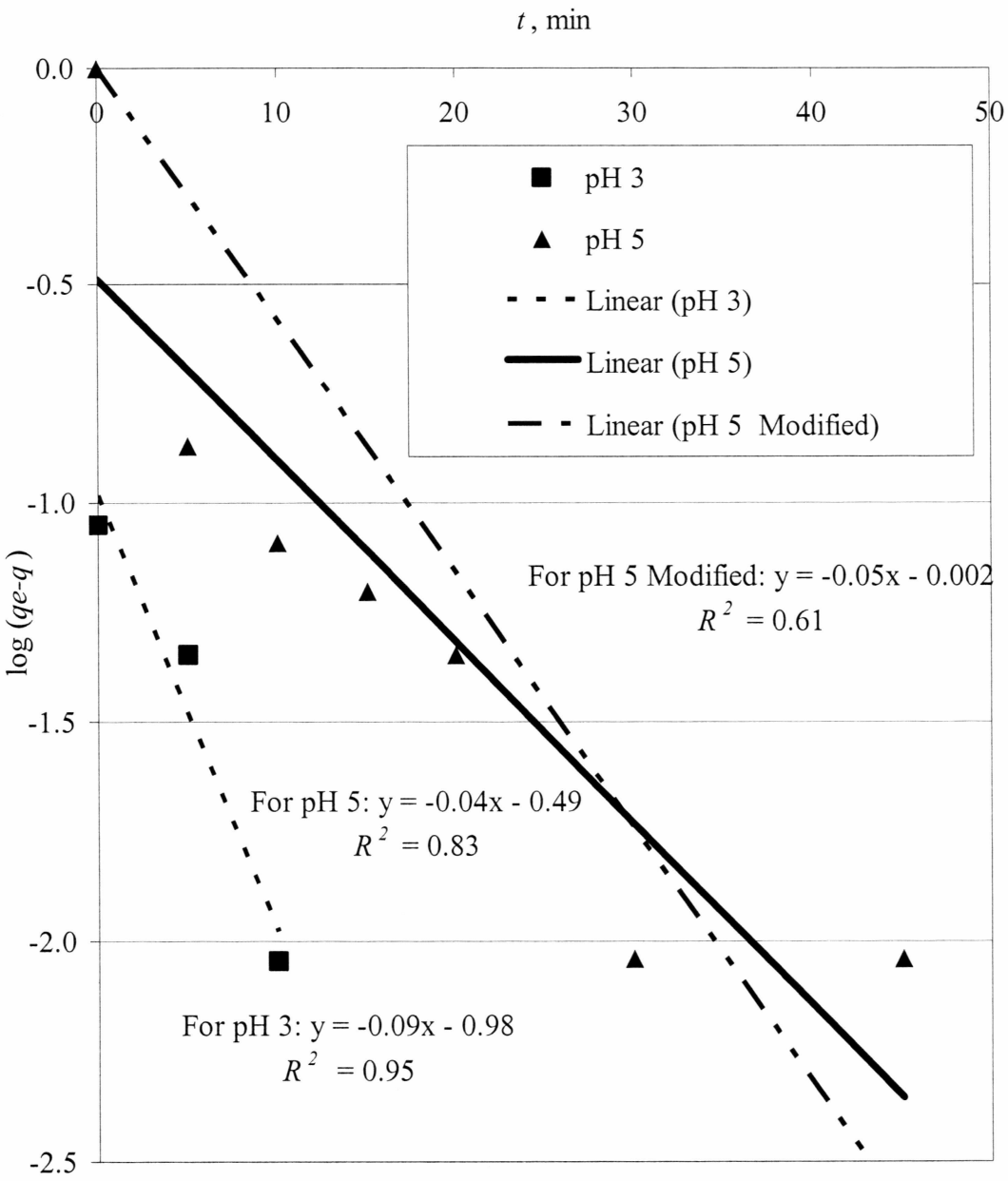

Figure 4.4: The modeling with the pseudo first-order kinetic model for pH 3 and 5

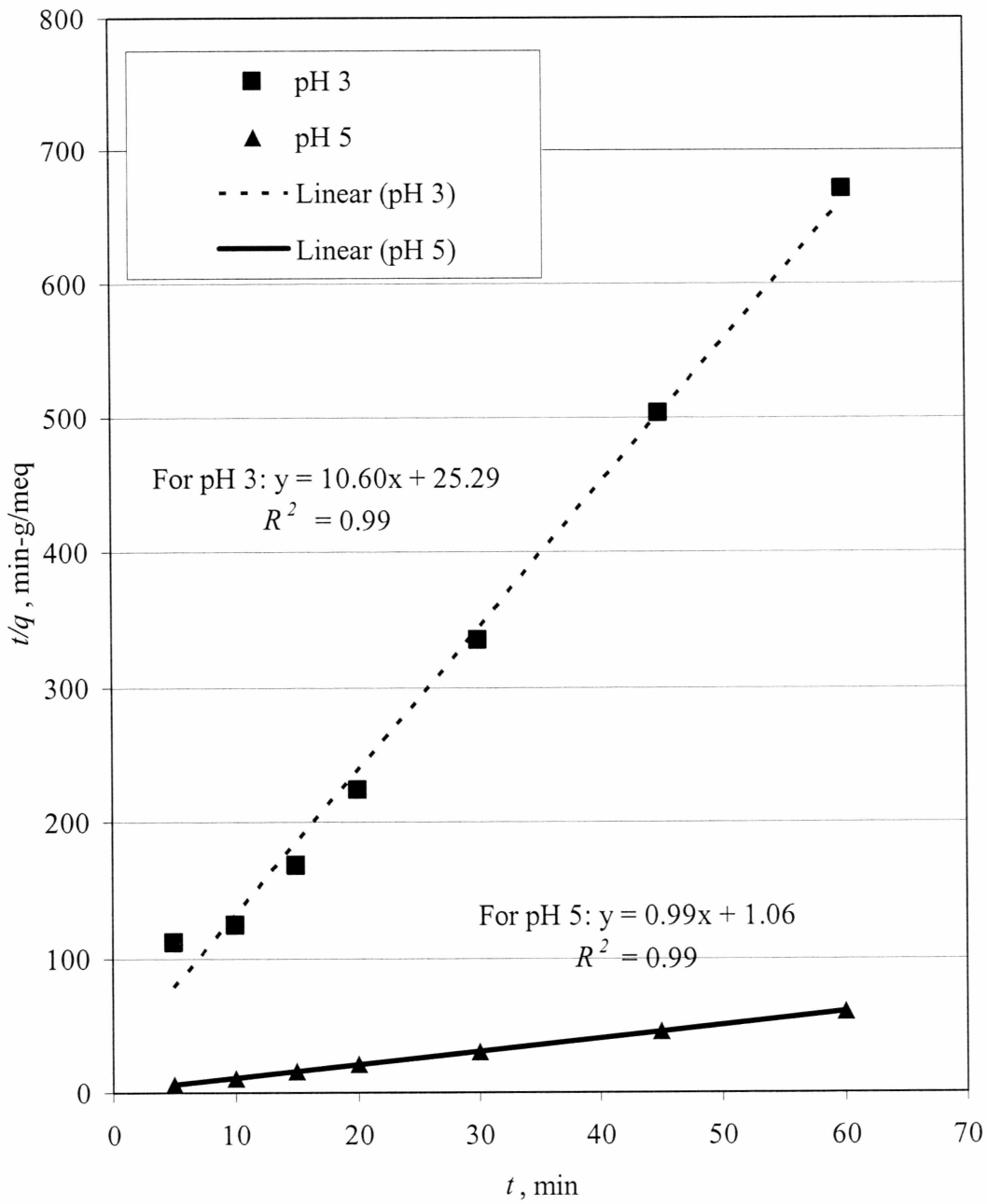

Figure 4.5: The modeling with the pseudo second-order kinetic model for pH 3 and 5

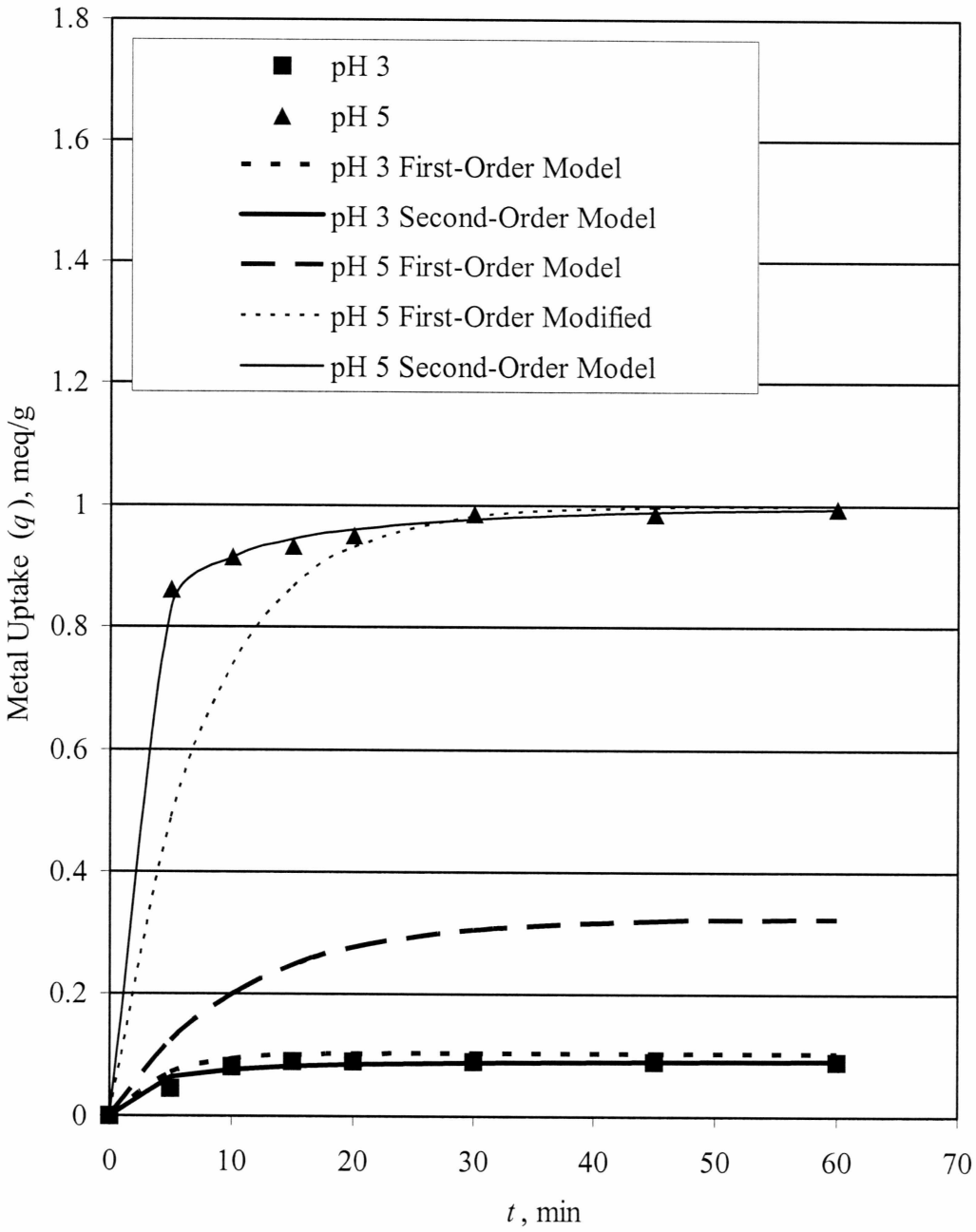

Figure 4.6: Metal uptake versus time for pH 3 and 5 with kinetic model curves

Table 4.2: Determination of rate constants and equilibrium metal uptake at pH 3 and 5

Model	pH	$k_{i,ads}$	*qe* (meq/g) Model	R^2	*qe* (meq/g) Experimental	*SSE/p*
First-order Kinetic	3	0.23 (min^{-1})	0.10	0.95	0.09	0.0022
	5	0.10 (min^{-1})	0.32	0.83	0.99	0.4171
	5 (*Modified*)	0.13 (min^{-1})	0.99	0.61	0.99	0.0217
Second-order Kinetic	3	0.57 (g/meq-min)	0.09	0.99	0.09	0.0000
	5	0.92 (g/meq-min)	1.01	0.99	0.99	0.0001

4.3.2 Effect of particle size on kinetics

The effect of biosorbent size on cadmium biosorption at pH 5 can be evaluated from Figure 4.9. The experimental results indicate that the biosorbent size influenced the metal uptake capacity and rate of cadmium biosorption. The particle sizes of 0.240 mm and 0.420 mm showed a shorter time of equilibration (45 min), compared with 90 min for 0.710 mm particles. The 0.240 mm size particle achieved the highest cadmium uptake. The metal uptake capacity for particle sizes of 0.420 mm and 0.710 mm was found to be lower than that for 0.210 mm particles. The rate constants ($k_{1,ads}$, $k_{2,ads}$) and *qe* (Table 4.3) for first and second-order reactions were calculated by using Equations 3.13 and 3.15, which are represented by straight lines plotted in Figures 4.7 and 4.8. The visual

inspection of straight lines in Figure 4.8, obtained by plotting *t/qe* versus *t* for different particle sizes, shows similar slopes yet different y-intercept values, which explain similar *qe* values but a higher rate constant for smaller particle sizes. The first and second-order kinetic models were used to fit the experimental data as can be seen in Figure 4.9. The experimental data followed second-order kinetics. The *SSE/p* ratio was almost negligible for the second-order kinetic model, whereas for the first-order kinetic model it was substantial for all three particle sizes (Table 4.3).

Slower uptake for larger particles was expected for a mass transfer controlled process (such as in this case), and it is necessary to point out that the three sizes of biosorbent were of different thicknesses (the dimension which determines the diffusion distance). The rate constants for particles of 0.240 mm and 0.420 mm were almost identical and considerably larger than for a particle of 0.710 mm diameter. The relatively higher metal uptake shown by the smallest particle size (0.240 mm) compared to larger particle sizes could be attributed to easy availability of a large surface area for sorption. The dependence of kinetics of metal uptake on particle size is observed from the data presented in Figure 4.9. The difference between times required to reach equilibrium between particle sizes 0.240 mm and 0.710 mm were clearer than those between particle sizes 0.240 mm and 0.420 mm.

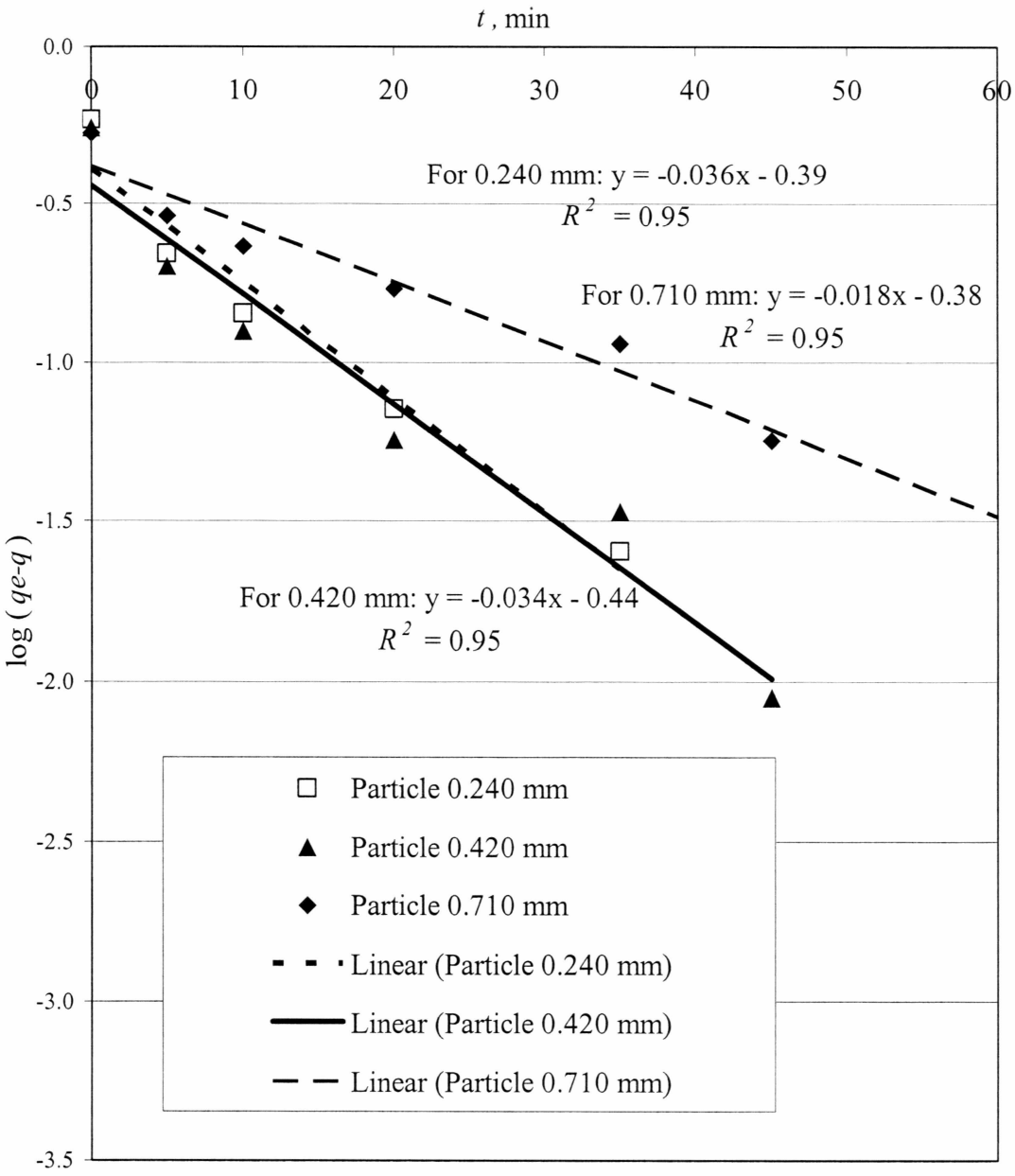

Figure 4.7: The modeling with pseudo first-order kinetic model for three particle sizes

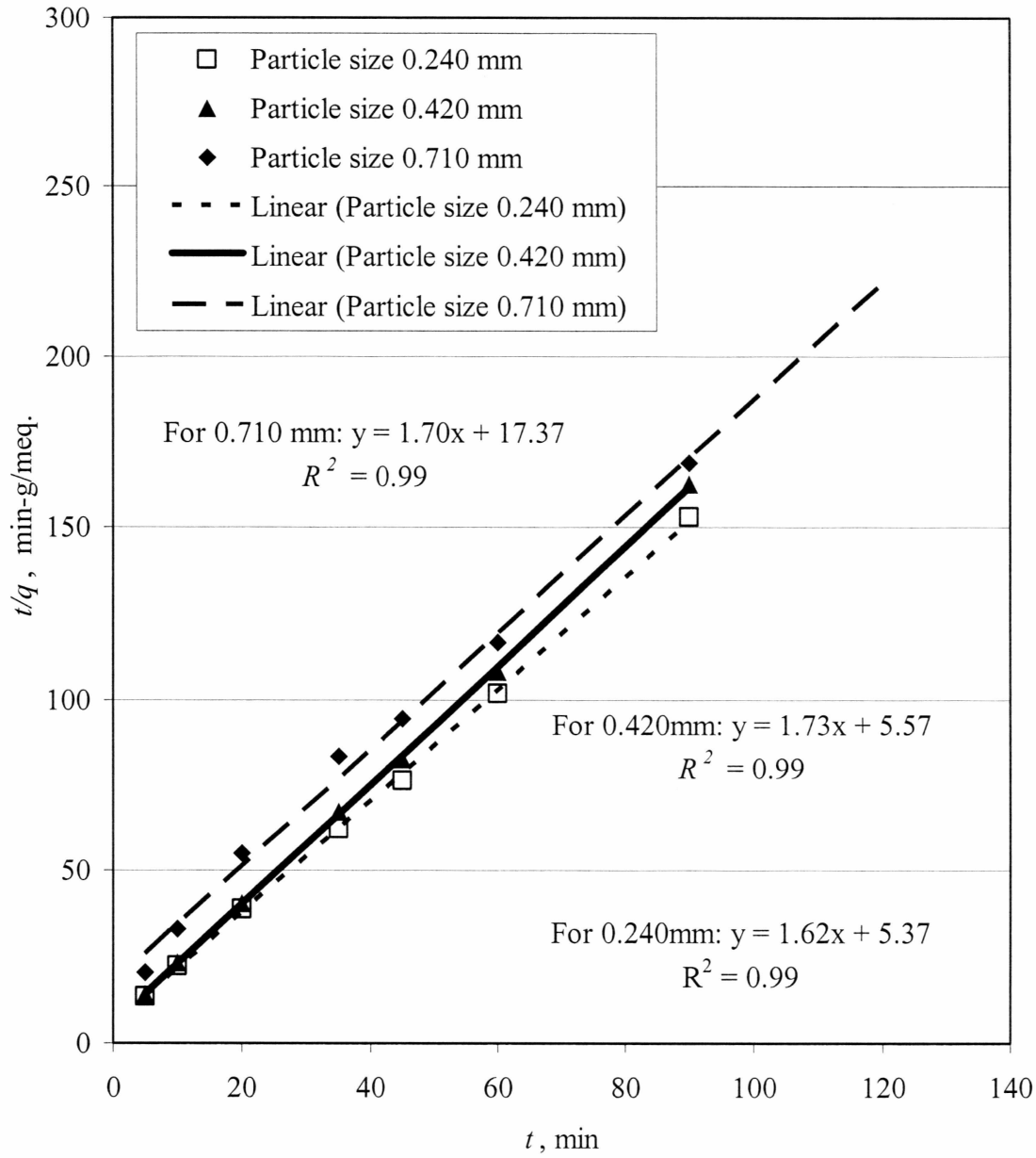

Figure 4.8: The modeling with pseudo second-order kinetic model for three particle sizes

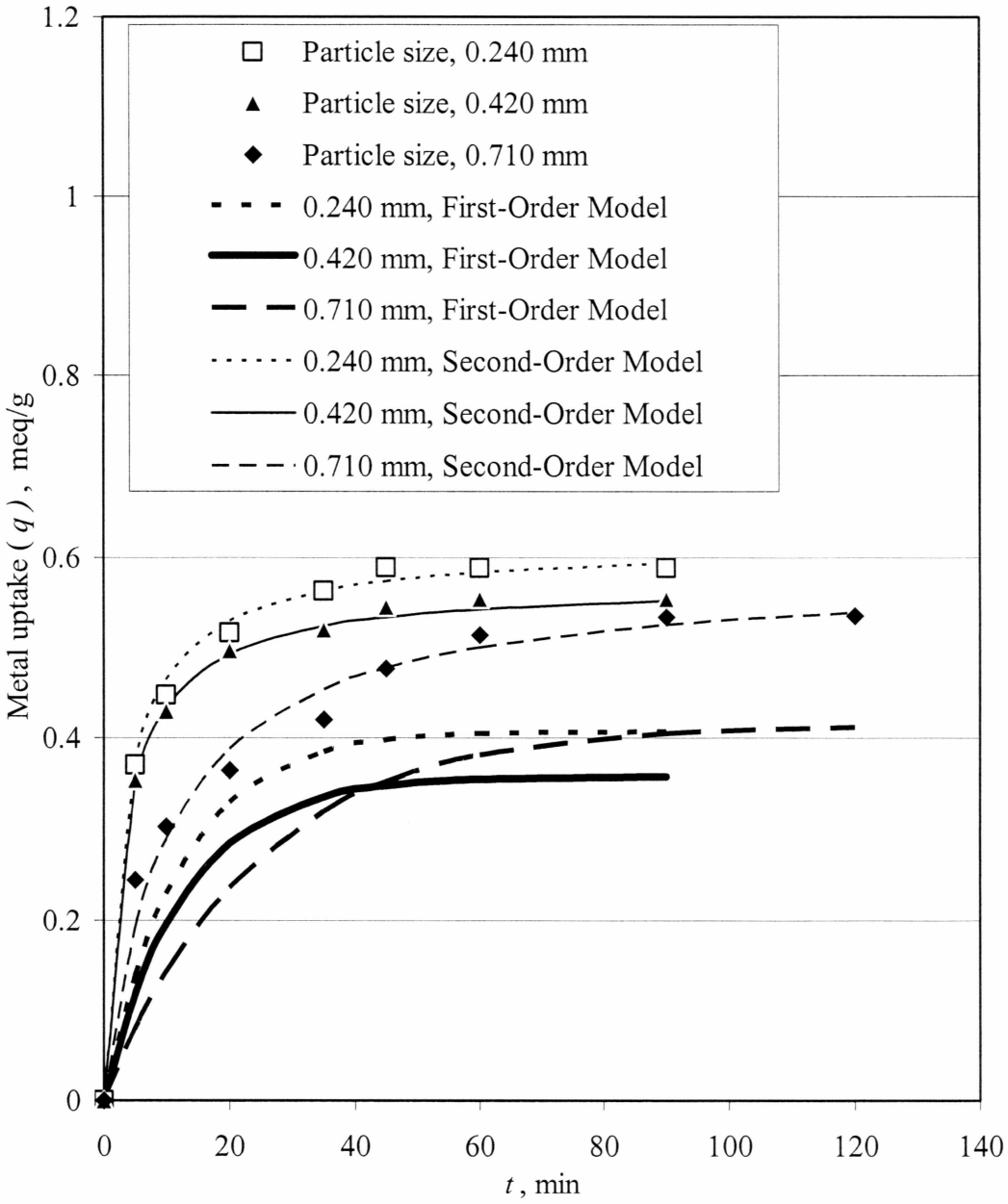

Figure 4.9: Metal uptake versus time for three different particle sizes at pH 5 with kinetic model curves

Table 4.3: Determination of rate constants and equilibrium metal uptake at pH 5 for different particle sizes

Model	Particle diameter mm	$k_{i,ads}$	*qe* (meq/g) Model	R^2	*qe* (meq/g) Experimental	*SSE/p*
First-order kinetic	0.24	0.07 (min^{-1})	0.41	0.95	0.58	0.0339
	0.40	0.08 (min^{-1})	0.36	0·95	0.55	0.0383
	0.71	0.043 (min^{-1})	0.41	0.95	0.53	0.0160
Second-order kinetic	0.24	0.50 (g/meq-min)	0.62	0.99	0.58	0.0004
	0.40	0.57 (g/meq-min)	0.54	0.99	0.55	0.0000
	0.71	0.17 (g/meq-min)	0.59	0.99	0.53	0.0005

4.4 Equilibrium studies and isotherm modeling

As described previously (section 4.1), the comparison of pectin-rich fruit materials led to the conclusion that citrus materials were more stable than apple residues and grape skins and could act as a potential candidate for biosorption. The stability criterion plays an important role when the same biosorbent material is used again in different cycles of heavy metal removal, i.e., in the case of multiple adsorption and desorption cycles.

The equilibrium studies at pH 3 and 5 for orange, grapefruit and lemon peels revealed higher metal uptake at pH 5 than at pH 3 occurred because of the lower proton concentration at pH 5 and thus decreased competition between protons and cadmium ions for the same binding site. For example, in the case of grapefruit peels, the maximum

metal uptake at pH 3 was 0.34 meq/L, while at pH 5 it increased to 0.49 meq/L (Table 4.4). The relationship between equilibrium uptake (*qe*) capacity and different final concentrations of cadmium was plotted in Figures 4.12, 4.13 and 4.14 for orange, grapefruit and lemon peels, respectively. As the final concentration of cadmium increased, equilibrium metal uptake started increasing but eventually it reached a plateau at higher concentrations of cadmium ion. The reason for occurrence of the plateau is the saturation of citrus peels (binding sites) with metal ions at higher concentrations. This observation is compatible with the Langmuir model.

Therefore, the modeling of these equilibrium data was carried out using the Langmuir isotherm. The parameters θ (equilibrium adsorption constant) and q_{max} were calculated from the intercept and slope of the plot of *Ce/qe* vs. *Ce* (Equation 3.19) in Figures 4.10 and 4.11 and these parameters are tabulated in Table 4.3. The modeled value of *qe* (Equation 3.18) was plotted with experimentally obtained equilibrium data in Figures 4.12-4.14. The Langmuir isotherm model seemed to fit some of the equilibrium data, but not those of orange peels and lemon peels at pH 3 and 5 (R^2 <0.9).

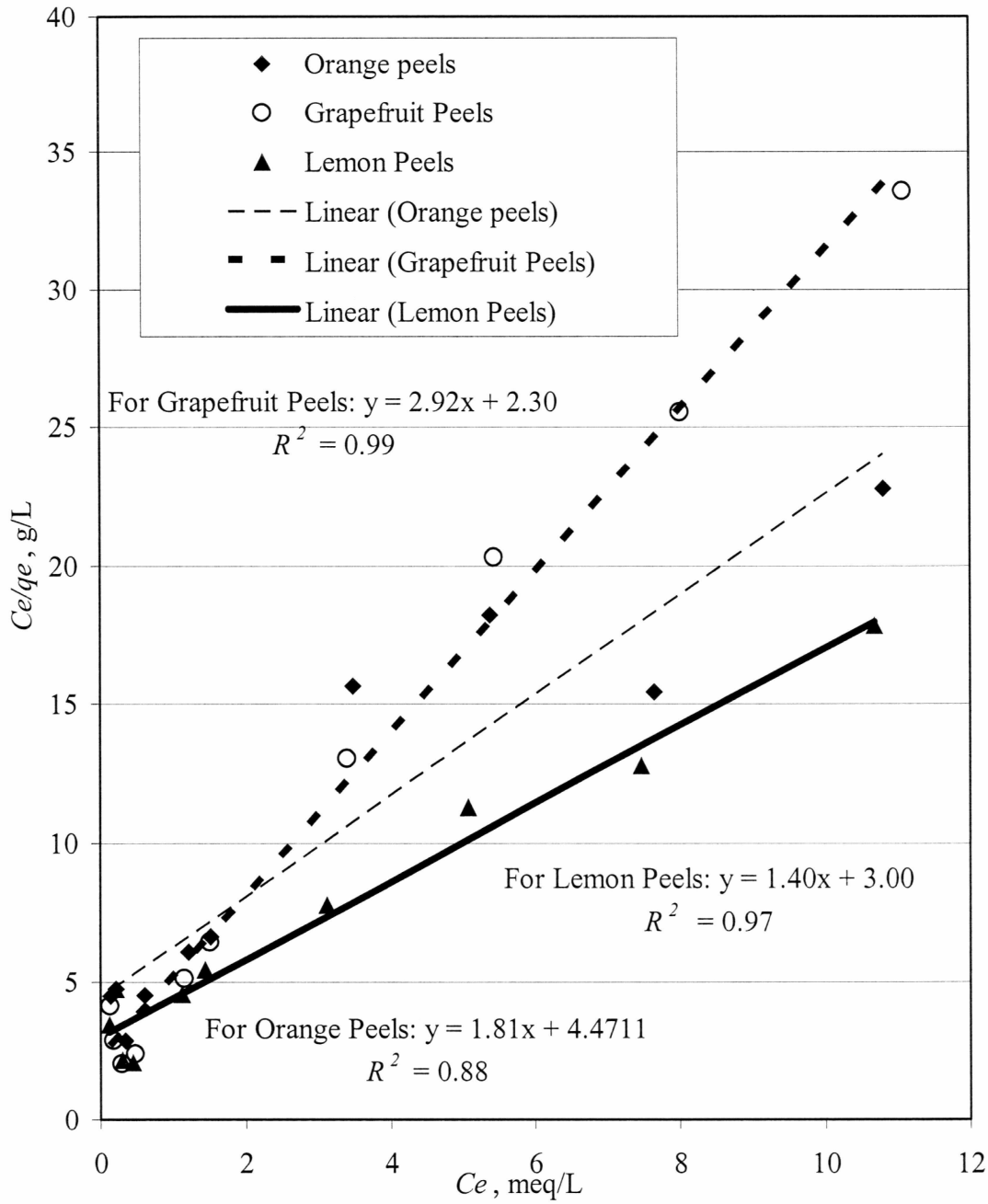

Figure 4.10: Plot of *Ce/qe* vs. *Ce* for pH 3 (linearized Langmuir Model)

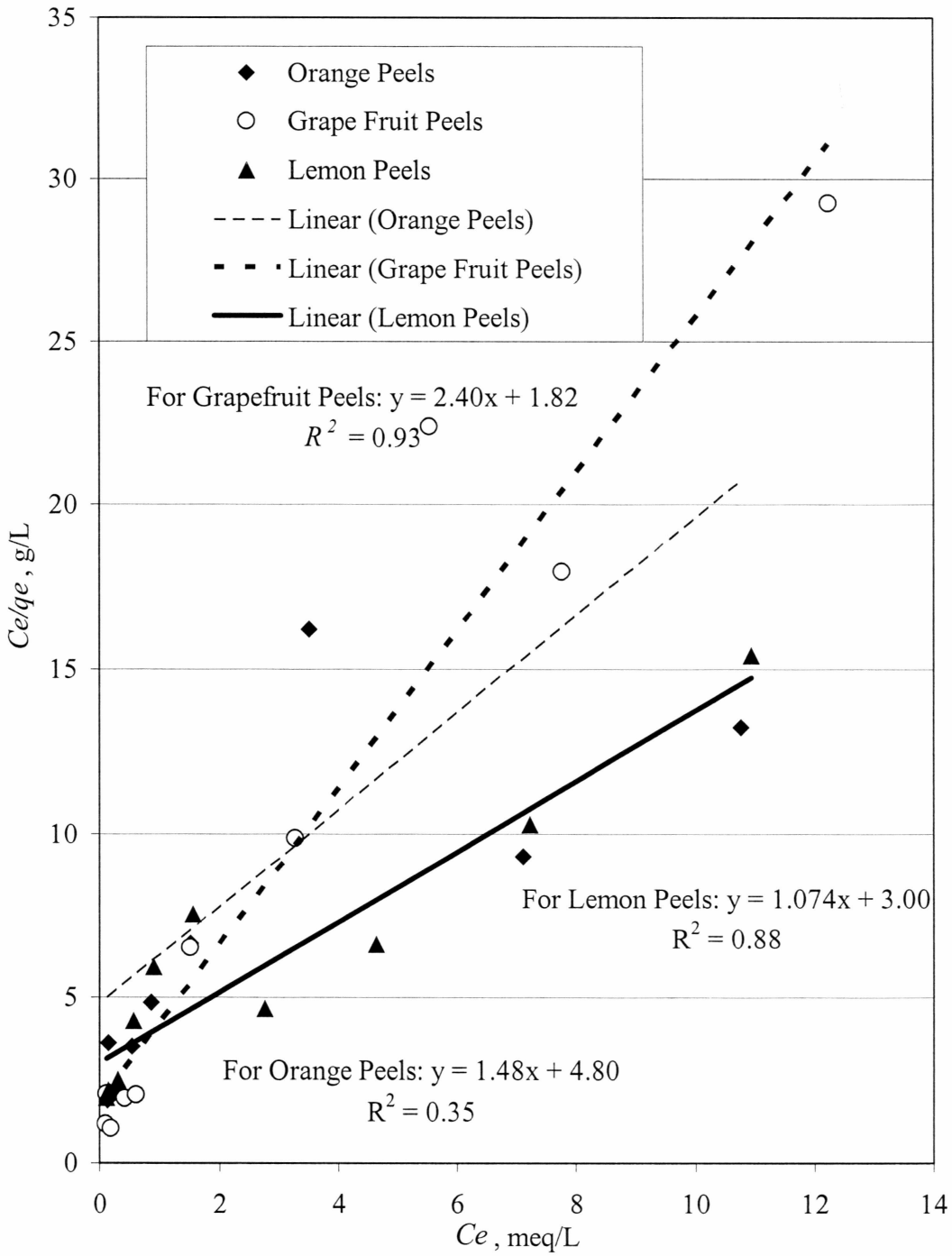

Figure 4.11: Plot of *Ce/qe* vs. *Ce* for pH 5 (linearized Langmuir Model)

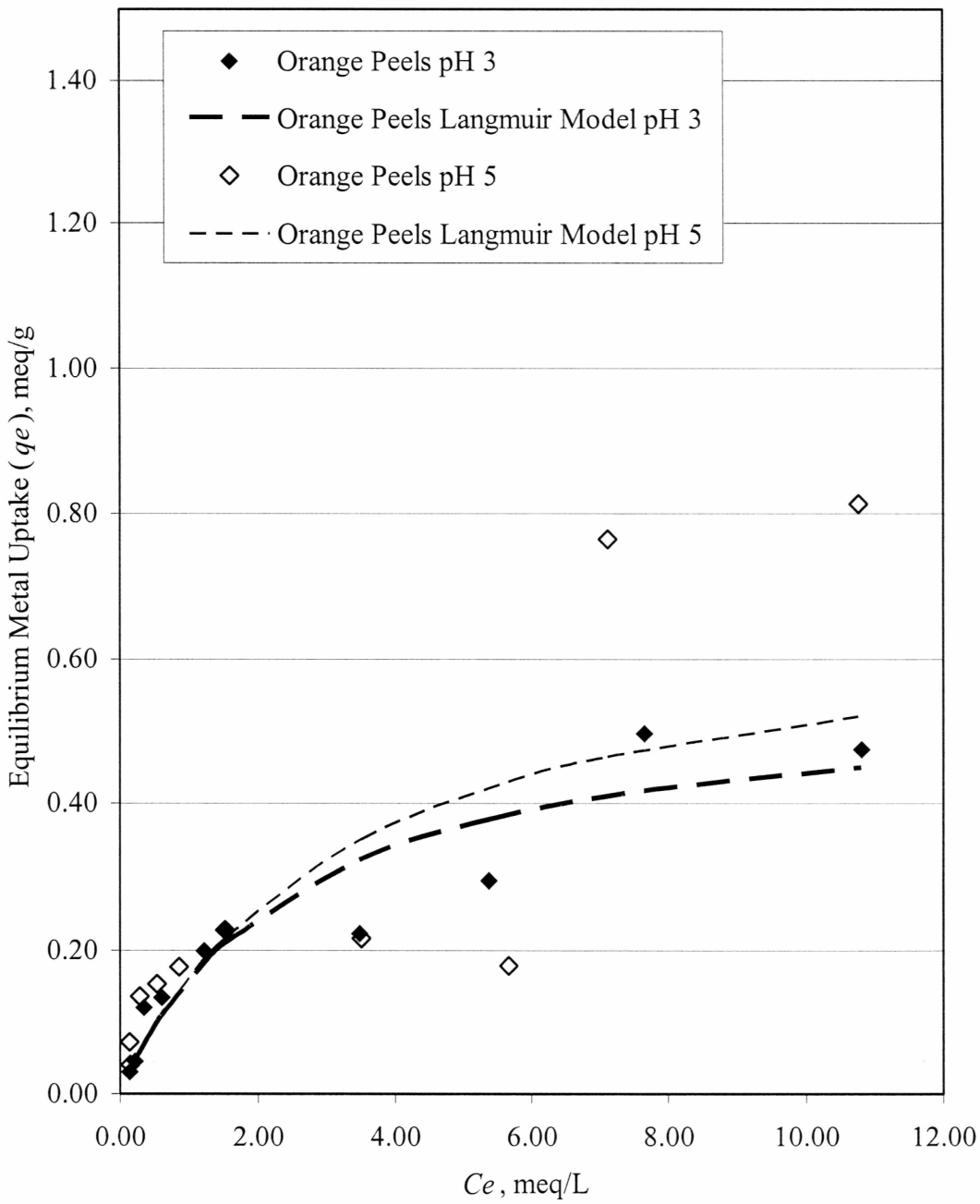

Figure 4.12: Langmuir modeling of orange peel data

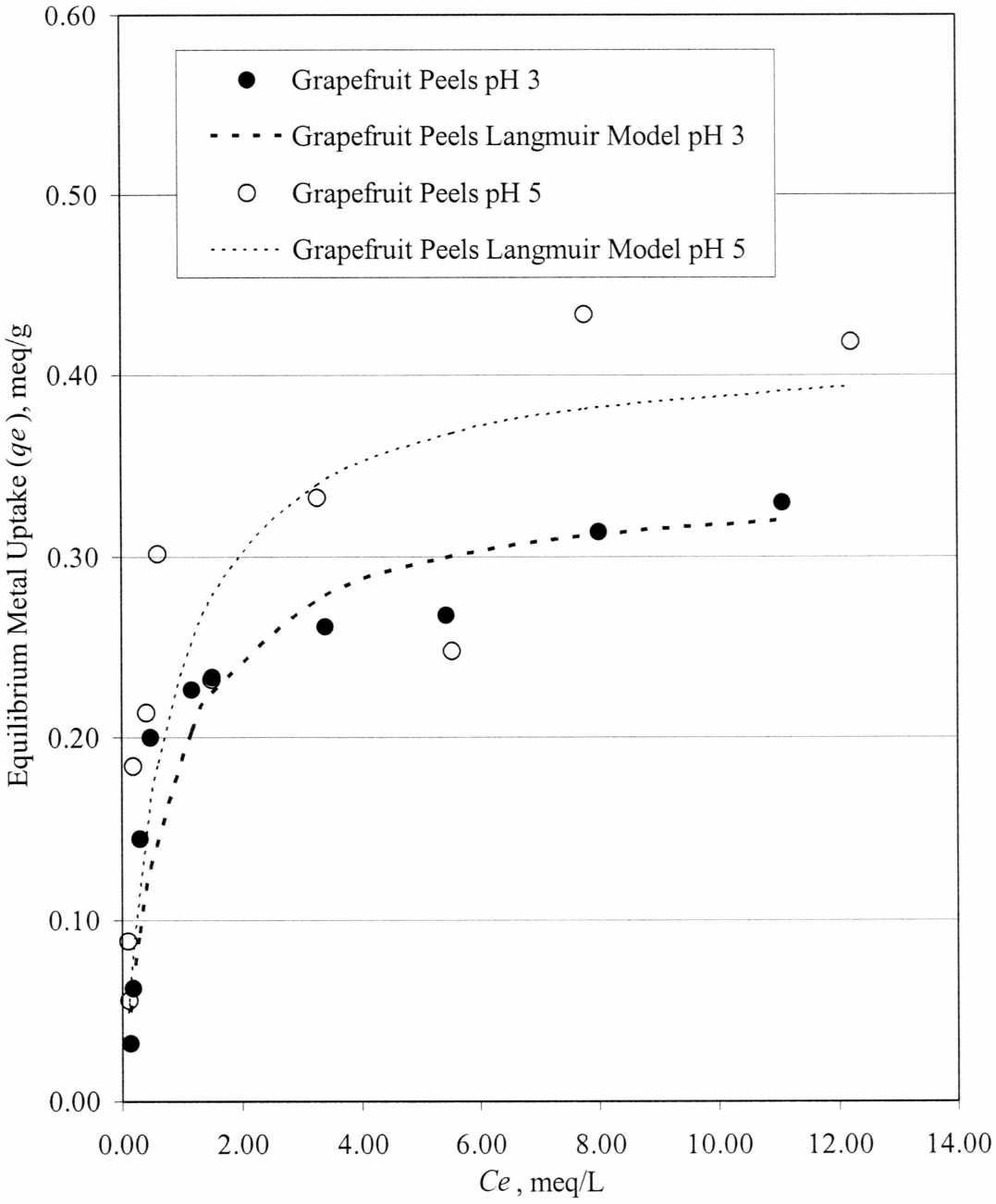

Figure 4.13: Langmuir modeling of grapefruit peel data

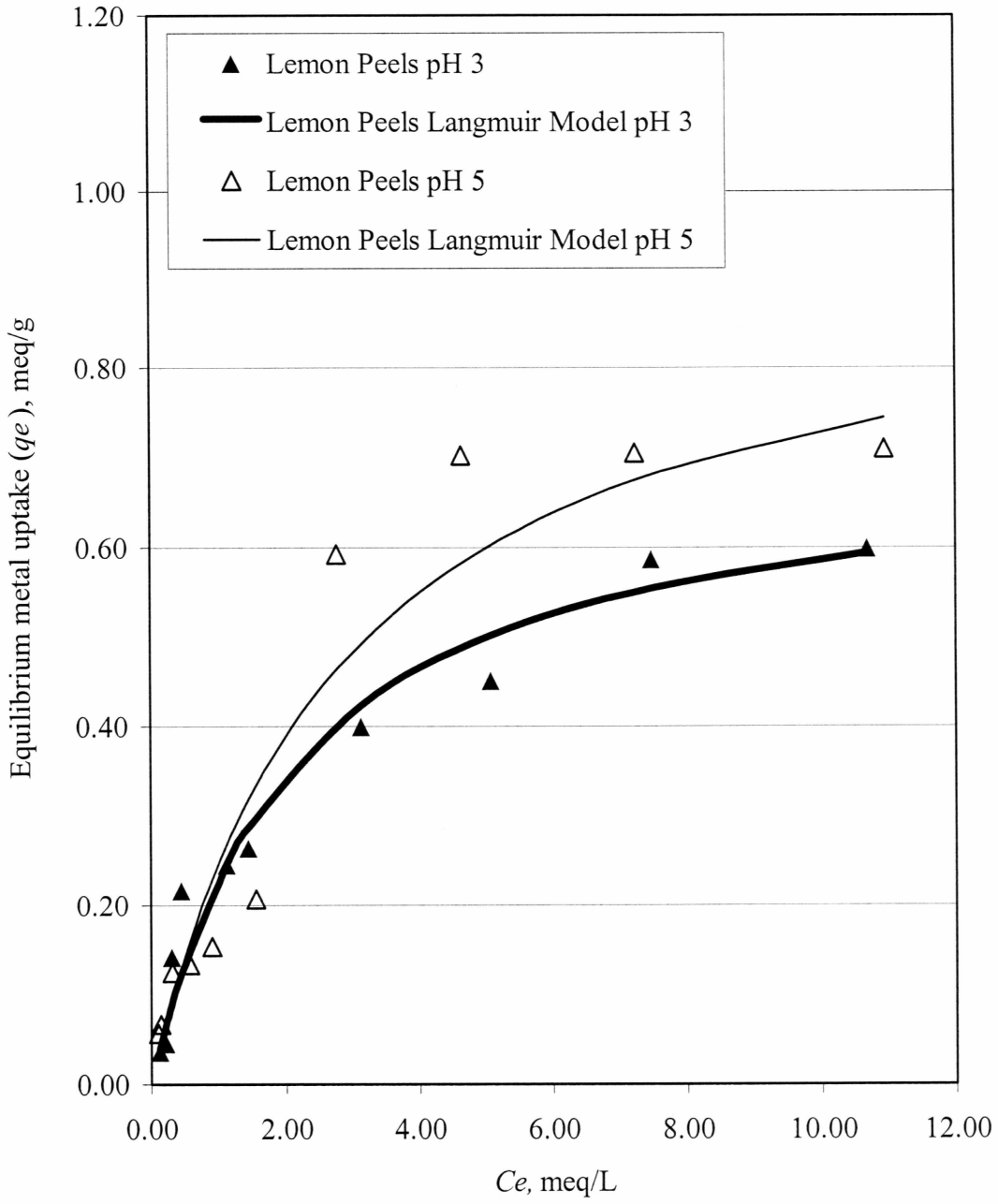

Figure 4.14: Langmuir modeling of lemon peel data

Table 4.4: Summary of Langmuir isotherm model parameters

	Langmuir Model Parameters				
	Biosorbent Material	θ (L/meq)	q_{max} (meq/g)	R^2	*SSE/p*
pH 3	Orange Peels *	0.40	0.55	0.88	0.003
	Grapefruit Peels *	1.27	0.34	0.99	0.001
	Lemon Peels *	0.46	0.71	0.97	0.002
	Protonated Lemon fruit waste using SAM **	0.50	0.86	0.90	0.001
pH 5	Orange Peels *	0.31	0.67	0.35	0.027
	Grapefruit Peels *	1.21	0.49	0.93	0.005
	Lemon Peels *	0.35	0.93	0.88	0.006
	Protonated Lemon fruit waste *	3.80	1.01	0.96	0.011
	Protonated Lemon fruit waste using SAM **	1.58	1.19	0.97	0.002

(* - $CdCl_2$, ** - $Cd(NO_3)_2$)

In equilibrium data for orange peels (Figure 4.12) as well as for lemon peels (Figure 4.14) at pH 3 and 5, two plateaus were observed. This anomalous behavior (more pronounced for orange peels than for lemon peels) could have been due to a combination of the following factors:

1. Two binding sites with different affinities for cadmium ions are present. The binding site for which cadmium ion had the strongest affinity became saturated at the first plateau and then cadmium ions started binding to a less favored binding site.
2. Heterogeneity of biosorbent material at different equilibrium points, i.e., "scattering" of data.

3. Formation of cationic complexation products (e.g. $CdCl^+$) which compete with cadmium ions in sorbing on the peels of orange and lemon. At pH 5, the concentration of Cd^{2+} is 53.61% of the total cadmium while that of $CdCl^+$ is 44.28% (Appendix C).

To screen out effects of the above mentioned factors on equilibrium uptake, the following changes were made to the experimental procedure:

1. A better defined sorbent material, lemon waste obtained from the fruit juice industry, was used. Due to prior processing (Sunkist®), this so called pectin peel material has different characteristics (e.g. higher pectin content, lower concentration of other constituents) compared to raw peels. The pectin peels were protonated before use.
2. Isotherm studies for protonated lemon fruit waste were carried out using SAM to eliminate the effect of biosorbent heterogeneity on the equilibrium data
3. Cadmium chloride salt was replaced by cadmium nitrate salt, since nitrate is not expected to form significant quantities of complexes with cadmium.

Typical smooth isotherms can be seen for protonated lemon peels using the conventional method and SAM, respectively, in Figures 4.15 and 4.16. Langmuir model was fitted to the data points and the Langmuir model parameters (θ and q_{max}) are tabulated in Table 4.4. The protonated lemon fruit waste showed an increase in sorption capacity when compared to that of non-protonated lemon peels (Figure 4.15). The elimination of hard

ions like Ca^{2+} and Mg^{2+} in the protonation process increased the affinity for cadmium. The use of protonated lemon fruit waste, with a higher pectin content than the untreated lemon peel (due to removal of soluble components), is likely to be responsible for the higher capacity. The equilibrium data obtained by the conventional method for protonated Lemon fruit waste using a $CdCl_2$ salt solution (Figure 4.15) showed a very similar metal uptake as obtained using SAM and $Cd(NO_3)_2$ salt (Figure 4.16). This means neither the experimental methodology (SAM or conventional) nor the anions used (Cl^- or NO_3^-) seem to have a strong effect on metal binding. This makes it unlikely that sorption of $CdCl^+$ complex was responsible for the S-shaped isotherm. The absence of anomalous behavior (S-shape), as observed in untreated lemon peels, in either case led to the conclusion that processing (protonation and leaching of soluble components) of lemon fruit waste decreased heterogeneity and increased pectin content of the biosorbent materials. This indicates that the anomalous behavior may have been due to involvement of several binding sites. However, additional research is necessary to compare binding sites in treated and untreated lemon peels. Use of SAM was found to be less time consuming, more reliable and more controllable than the conventional experimental procedure, and the effect of sorbent heterogeneity was completely removed. The Langmuir model was used to fit data in Figures 4.15 and 4.16 and to evaluate θ and q_{max} (Table 4.4). At both pH values q_{max} was higher for protonated lemon waste than raw lemon peels.

The pH-sensitive isotherm (Equation 3.26) was used to fit experimental data obtained by SAM. The unknown parameters were determined by using the curve fitting toolbox

(Matlab®). It was observed that solutions for the pH-sensitive model became unstable as the number of parameters to be fitted increased. To minimize instability, only one binding site was considered and the proton binding constant (K_{CH}) for this site was assumed to be $10^{3.8}$ (refer to section 4.2) as the carboxyl group is the main group involved in acid base reactions between pH 3 and 5. However, since the actual metal binding is likely to take place at several sites, the site quantity was adjusted to fit the experimental data rather than assuming the carboxyl site quantity obtained from titrations (section 4.2). Figure 4.17 shows the plots for the pH-sensitive isotherm model for pH 3 and 5. K_{LM} and L_T were fitted specifically to predict the sorption data at these pH values. In addition to that, a model prediction for pH 5 is shown assuming constant K_{LM} (obtained from fitting for pH 3) and only determining L_T for pH 5, since K_{LM} should be constant for both pH values if pH effects are actually to be predicted. The curve fitting parameters can be found in Table 4.5. The values of total site concentrations apparently have been over-predicted by this model compared to the site quantities obtained by titration (Table 4.1). To make the model more realistic, additional constraints may have to be placed on the total number of metal binding sites so that it does not exceed the total amount of functional groups. The presence of other binding sites (in this case pK_{a2} and pK_{a3}) can not be ignored in pH-sensitive ion exchange modeling, only the results for modeling with one site are shown here. Adding more terms for other site on the right hand side of Equation 3.26 leads to a total of 4 unknown parameters, which in turn result into either unstable solutions or very poor fit to the data.

Table 4.5: pH-sensitive ion exchange model parameters (for single site only), assuming $pK_{CH1} = 3.8$

pH	K_{LM} (L/mol)	L_T (mmol/g)	R^2	*SSE/p*
3	199.50	6.98	0.93	0.004
5	401.20	2.45	0.97	0.011
5 (constant K_{LM} obtained from pH 3)	199.50	2.89	0.95	0.001

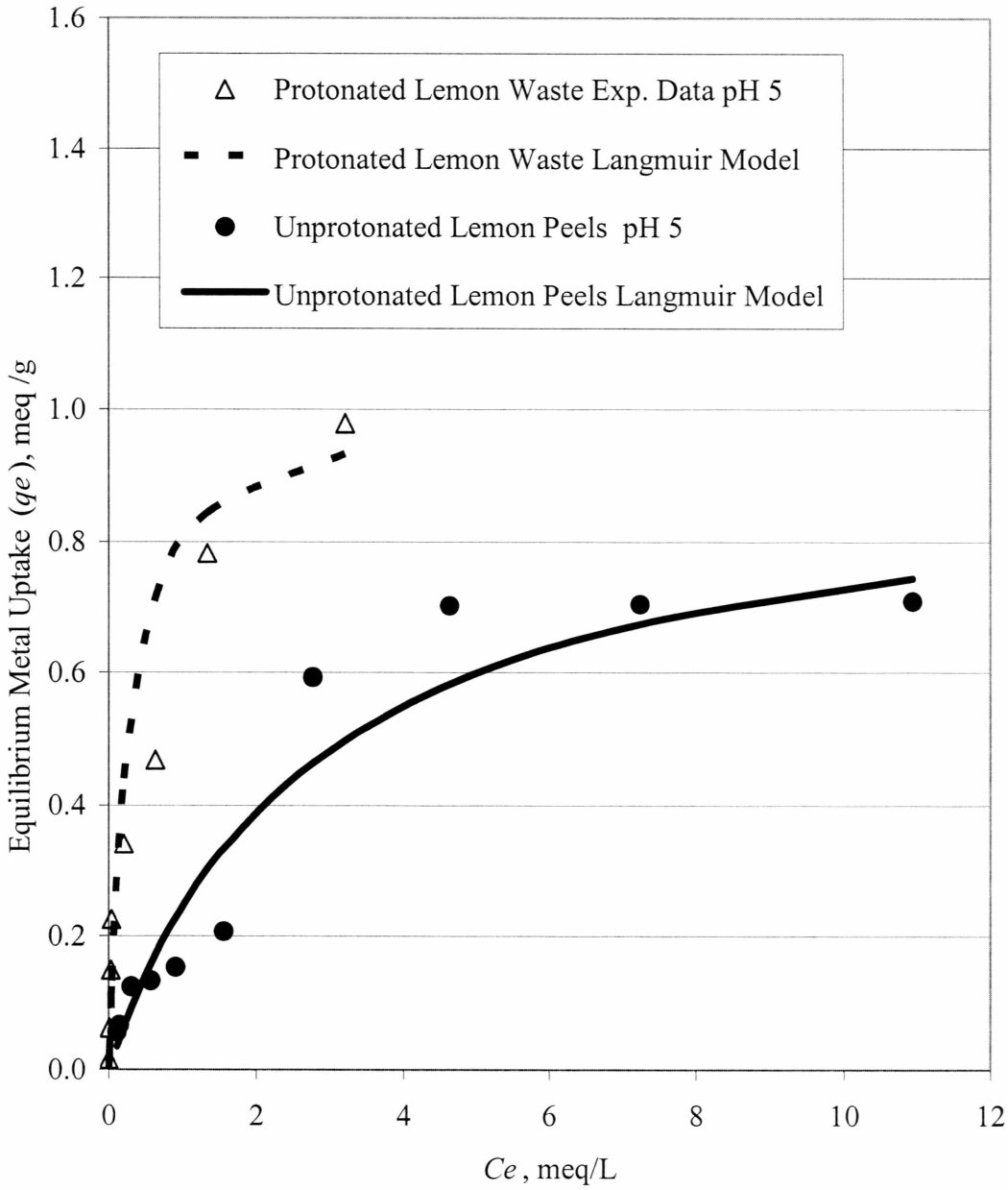

Figure 4.15: Comparison between protonated lemon fruit waste and non-protonated lemon peels using Langmuir modeling (with $CdCl_2$ solutions)

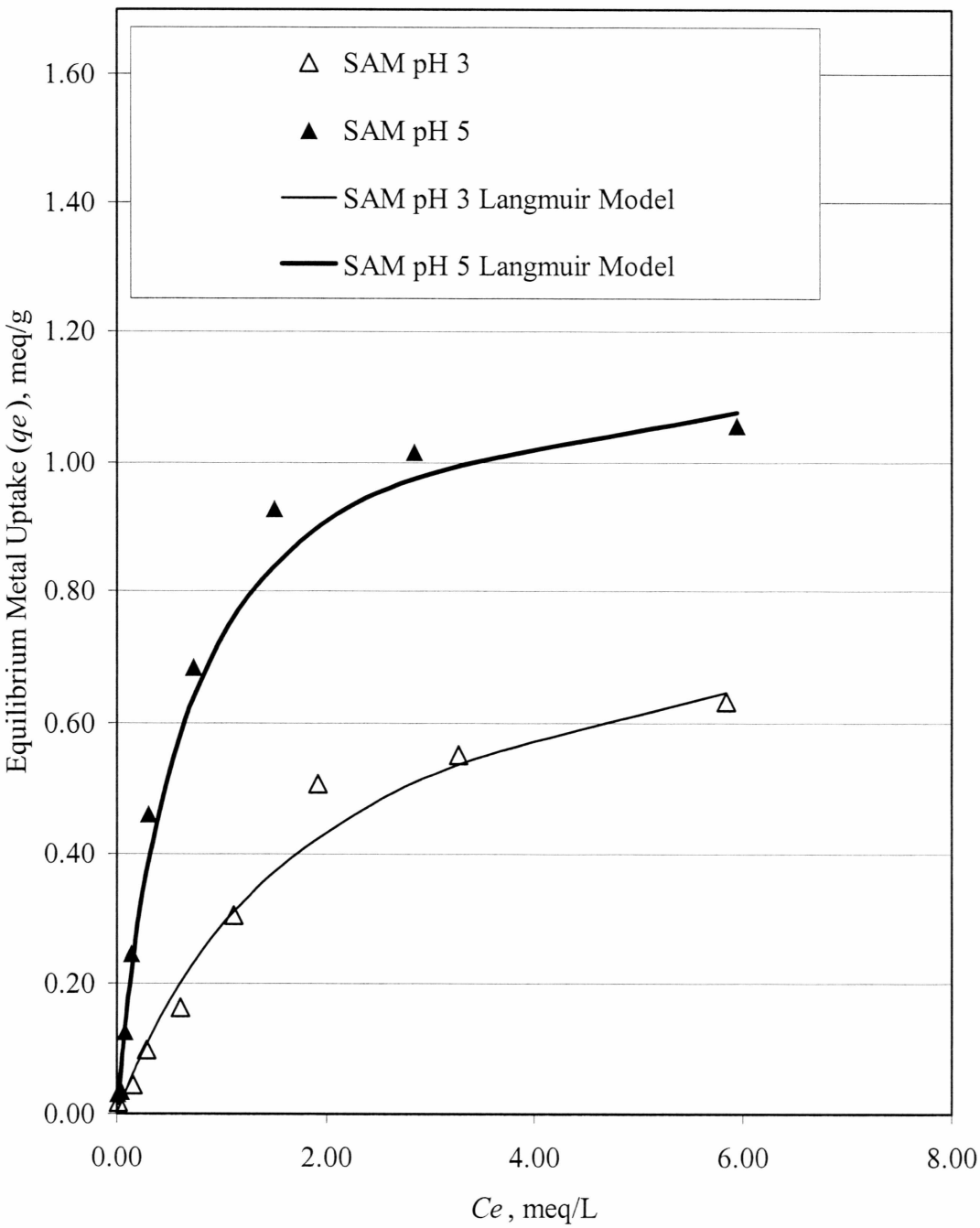

Figure 4.16: Langmuir modeling for lemon fruit waste (SAM) data using $Cd(NO_3)_2$ solution

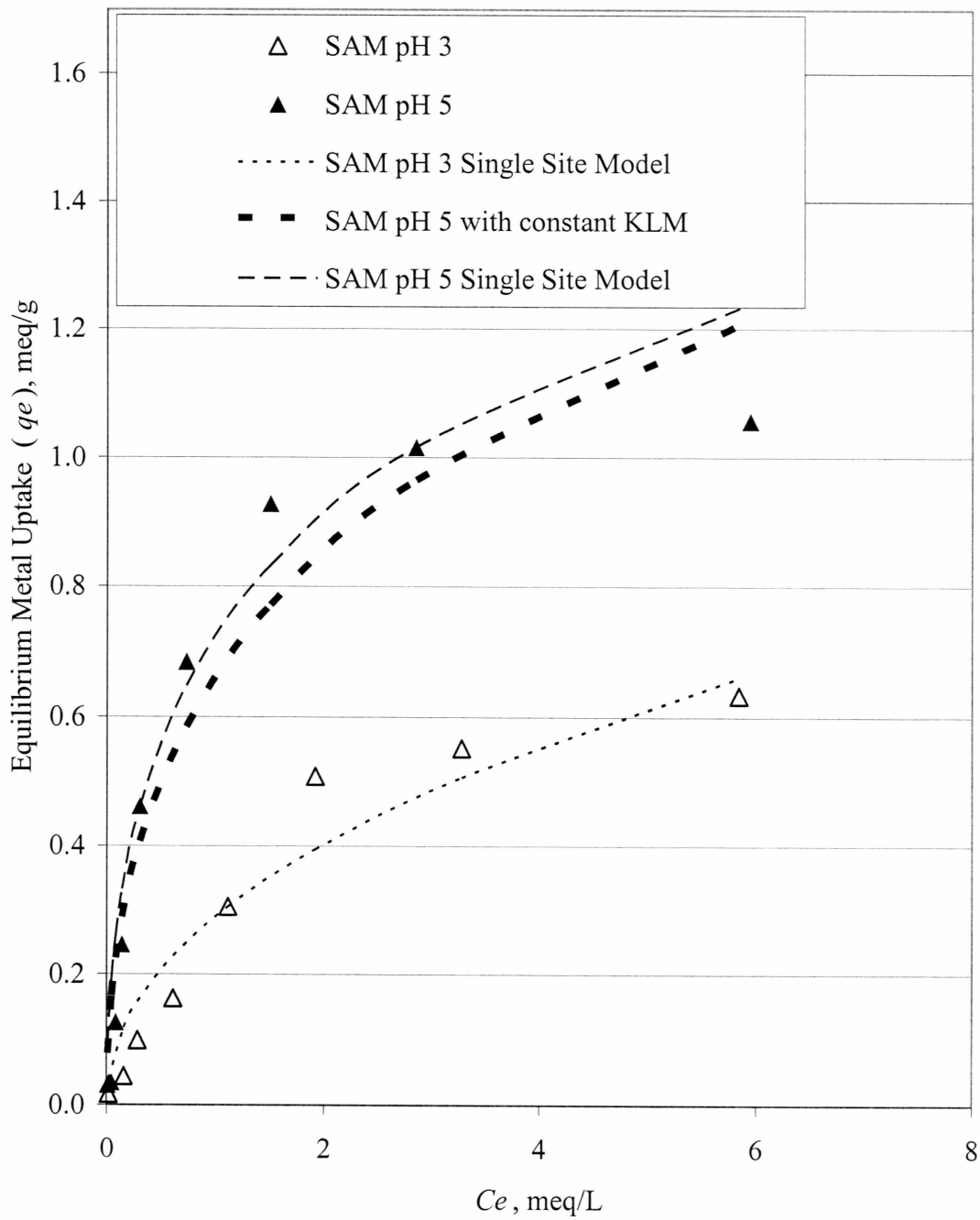

Figure 4.17: pH-sensitive ion exchange model with Langmuir modeling for lemon fruit waste (SAM) data

Chapter 5

Conclusions and Recommendations

5.1 Conclusions

- From this biosorption study of pectin-rich fruit materials using cadmium as the metal ion, it was concluded that citrus peels are suitable for biosorption due to good uptake and the fact that they were more stable than apple residues and grape skins. This supports hypothesis one.
- The presence of carboxyl groups and other unknown acidic sites in lemon fruit waste was confirmed by potentiometric titration using a continuous pK_a spectrum technique for data interpretation, supporting hypothesis two.
- An increase in metal uptake capacity was observed at higher pH values, indicating the competition of protons for binding to acidic sites at low pH. The metal uptake rate increased as particle size decreased, which can be regarded as an indication of mass transfer limitations (hypothesis 3).
- Protonation and the technique called subsequent additions method (SAM) increased sorption capacity and decreased heterogeneity of biosorbent materials respectively, providing additional support for hypothesis 1, which states that citrus peels are good biosorbents.
- Using untreated peels, anomalous S-shaped isotherms were observed. Apparently this behavior was due to sorbent heterogeneity and / or the involvement of several

binding sites of the untreated peels, since no such behavior was observed for protonated waste.

- The Langmuir isotherm was able to fit most equilibrium data (hypothesis 4).
- The pH-sensitive expanded isotherm could model the effect of pH on cadmium uptake (hypothesis 4).
- The pectin-rich citrus fruit material is a potential candidate for biosorption and more studies in this area will help to evaluate economical use of this fruit waste material.

5.2 Recommendations

The same equilibrium studies could be performed at different ionic strengths (0.01 M, 0.1M and 1M) to understand the effect of ionic strength on metal binding at pH 3 and 5.

To investigate effect of metal concentration on kinetics, experiments could be carried out by changing initial concentration of metal at constant pH and particle size and a kinetic model, which takes the effect of metal concentration into account, has to be used.

More studies can be carried using FTIR to determine the nature of different binding sites, results of which will corroborate the pK_a spectrum developed in this study.

Two metal or multi metal systems (for e.g. Cd^{2+}, Cu^{2+}) should be studied to understand the effect of one metal ion on the other at different pH values and a selectivity scale should be developed.

More in-depth investigations should be conducted to confirm the cause for anomalous isotherms. The raw citrus peels and protonated pectin peels have to be better characterized by identifying functional groups. Possible sorption of metal-ligand complexes has to be investigated by using different anions (e.g. NO_3^-, Cl^-) under different conditions (untreated citrus peels with NO_3^- and Cl^-, protonated pectin peels with NO_3^- and without SAM).

Chapter 6

References

Ajaml, M.; Khan-Rao R. A.; Ahmad, R.; Ahmad, J. (2000) Adsorption studies of *Citrus reticulata* (fruit peel of orange): removal of Ni (II) from electroplating wastewater. *Journal of Hazardous Materials.* 79, 117-131.

Annadurai, G.; Juang, R. S.; Lee, D. J. (2003) Adsorption of heavy metals from water using banana and orange peels. *Water Science and Technology.* 47, 185-190.

Antunes, W. M.; Luna, A. S.; Henriques, C. A.; da Costa, A. C. A. (2003) An evaluation of copper biosorption by a brown seaweed under optimized conditions. *Journal of Biotechnology.* 6, 1-11.

Atkinson, B. W.; Bux, F.; Kasan, H. C. (1998) Considerations for application of biosorption technology to remediate metal-contaminated industrial effluents. *Water South Africa.* 24, 129-126.

Brassard, P.; Kramer, J. R.; Collins, P. V. (1990) Binding site analysis using linear programming. *Environmental Science & Technology.* 24. 195-201.

Buffle, J. (1990) Complexation of reactions in aquatic systems-An analytical approach. *Ellis Horward Limited.*

Cernik, M.; Borkovec, M.; Westall, J. C. (1995) Regularized Least-Squares Methods for the calculations of discrete and continuous affinity distributions for heterogeneous sorbents. *Environmental Science & Technology.* 29, 413-415.

Chen, J.P.; Wang, L. (2001) Characterization of a Ca-alginate based ion-exchange resin and its applications in lead, copper, and zinc removal. *Separation Science & Technology.* 36(16), 3617–3637.

Cohen-Shoel, N.; Ilzycer, D.; Gilath, I.; Tel-Or E. (2002) The involvement of pectin in Sr^{2+} biosorption by *Azolla. Water Air and Soil Pollution.* 125, 195-205.

Cossich, E. S.; Tavares, C. R. G.; Ravagnani, T. M. K. (2002) Biosorption of chromium (III) by *Sargassum* sp. biomass. *Journal of Biotechnology.* 5, 133-140.

Davis, T. A.; Volesky, B.; Alfonso, M. (2003) A review of the biochemistry of heavy metal biosorption by brown algae. *Water Research.* 37, 4311-4330.

Dronnet, V. M.; Axelos, M. A. V.; Renard, C. M. G. C.; Thibault, J. F. (1996) Characterization and selectivity of divalent metal ion binding by citrus and sugar beet pectin. *Carbohydrate Polymer.* 30, 253-263.

Dronnet, V. M.; Renard, C. M. G. C.; Axelos, M. A. V.; Thibault, J. F. (1997) Binding of divalent metal cations by sugar-beet pulp. *Carbohydrate Polymers.* 34, 73-82.

Genialab (2002). Website of the Genialab Company on pectin properties and sources: *http://www.genialab.de/inventory/pectinate.htm.*

Grant, G. T.; Morris, E. R.; Rees, D. A.; Smith, P. J. C.; Thom, D. (1973) Biological interactions between polysaccharides and divalent cations: The egg-box model. *FEBS Letters.* 32, 195-198.

Harel, P.; Mignot, L.; Sauvage, J. P.; Junter, G. P. (1998) Cadmium removal from dilute aqueous solution by gel beads of sugar beet pectin. *Industrial Crops and Products.* 7, 239-247.

Jumle, R.; Narwade, M. L.; Wasnik, U. (2002) Studies in adsorption of some toxic metal ions on *Citrus sinesis* skin and *Coffea arabica* husk: Agricultural by product. *Asian Journal of Chemistry.* 14, 1257-1260.

Kartel, M. T.; Kupchik, L. A.; Veisov, B. K. (1999) Evaluation of pectin binding of heavy metal ions in aqueous solutions. *Chemosphere.* 38, 2591-2596.

Kohn, R. (1987) Binding of divalent cations to oligomeric fragments of pectin. *Carbohydrate Research.* 160, 343-353.

Lee, S. H.; Shon, S. J.; Chung ,H.; Lee, M-Y.; Yang, J-W. (1999) Effect of chemical modification of carboxyl groups in apple residues on metal ion binding. *Korean Journal of Chemical Engineering.* 16, 576-580.

Maranon, E.; Sastre, H. (1992) Behavior of lignocellulosic apple residues in the sorption of trace metals in packed beds. *Reactive Polymers.* 18, 173-176.

Pangnanelli, F.; Papini, P. M.; Toro, M.; Veligo, F. (2000) Biosorption of metal ions on *Arthrobactor* sp.: Biomass characterization and biosorption modeling. *Environmental Science & Technology.* 33, 2773-2778.

Reddad, Z.; Gerente, C.; Andres, Y.; Le Cloirec, P. (2002) Modeling of single and competitive metal adsorption onto a natural polysaccharide. *Environmental Science & Technology.* 36, 2242-2248.

Schiewer, S.; Volesky, B. (1995) Modeling of the proton-metal ion exchange in biosorption. *Environmental Science & Technology.* 29, 3049-3058.

Smith, S. D.; Ferris, G. F. (2001) Proton binding by hydrous ferric oxide and aluminum oxide surfaces interpreted using fully optimized continuous pK_a spectra. *Environmental Science & Technology.* 35, 4637-4642.

Smith, S. D.; Adams, N. W. H.; Kramer, J. R. (1999) Resolving uncertainty in chemical speciation determinations. *Geochimica et Cosmochimica Acta.* 63, 3337-3347.

Synytsya, A.; Copikova, J.; Matejka, P.; Machovic, V. (2003) Fourier transform Raman and infrared spectroscopy of pectins. *Carbohydrate Polymers.* 54, 97-106.

Vincent (2001) Website of Vincent Corporation on production of pectin peels. *http://www.vincentcorp.com/tech_papers/fmc2_sg.html.*

Volesky, B. (1999) Sorption and Biosorption - Chapter 6: Evaluation of biosorption performance. *ISBN 0-9732983-0-8*, 103-178.

Volesky, B. (2003) Biosorption: Application aspects–Process simulation tools. *Hydrometallurgy.* 71, 179-190.

Yang, J. and Volesky, B. (1999) Biosorption and elution of uranium with seaweed biomass: *Biohydrometallurgy and the Environment Toward the Mining of the 21st Century,* Internet. Biohydrometallurgy Symposium Proceedings, 1999, volume B, Ballester, A. & Amils, R. (eds.) Elsevier Sciences, Amsterdam, The Netherlands. 483-492.

Yun, Y-A.; Park, D.; Park, J. M.; Volesky, B. (2001) Biosorption of trivalent chromium on the brown seaweed biomass. *Environmental Science & Technology.* 35, 4353-4358.

Appendix A

Matlab® Codes for FOCUS

The following Matlab® codes were obtained from Dr. Smith (Wilfrid Laurier University, Canada). The codes were slightly modified for this study.

1. Matlab® Command

```
[pH, b, origin, p0] = return_data_for_process (pH, b, maxpH, minpH, pKs, Lts, So);
lambdaguess 1;
OPTIONS = optimset ('fminsearch');
best_lambda = fminsearch ('minimize_distance', lambdaguess, OPTIONS, p0, pH, b,
origin, pKs);
[distance,BestLts] = minimize_distance (best_lambda, p0, pH, b, origin, pKs);
```

2. Regularized fitting code

```
function [II, GG, HH] = regularized_fitting (pH, b, pKs, p, lambda, flag)
% Make a matrix (A) add a site with zero concentration on either end
delta = pKs (2) – pKs (1); [n,m] = size(pKs);
pKs_mod = [pKs (1) - 3*delta pKs (1) - 2*delta pKs (1)-delta pKs pKs (m) + delta pKs
(m) + 2*delta pKs (m) + 3*delta];
K = 10 ^ (-1*pKs_mod); H = 10^ (-1*pH);
for i = 1:size (pH,1)
    for j = 1:size (pKs_mod,2)
        A (i, j) = K (j)/ (K (j) + H (i));
    end
```

```
end
OPTIONS = []; OPTIONS (14) =250000000; OPTIONS (1) = 1;
OPTIONS (2) = 1e-5; OPTIONS (3) = 1e-5;
OPTIONS (16) = 1e3*eps; OPTIONS(17) = 1e6*eps;
OPTIONS (6) = 0;
OPTIONS (7) = 0;
[n, m] = size (p); vlb = [zeros (n, m-1) -inf]; vub = + inf*ones (size (vlb));
%vub = 100*ones (size (vlb));
if flag = = 0
x = constr ('fast_regularized_error', p, OPTIONS, vlb, vub, [], pKs_mod, A, b, pH,
lambda, 0);
p = x; chi2 = []; R = [];
end
% and plot
if flag = = 1;
  [err, dummy,chi2,R] = fast_regularized_error (p, pKs_mod, A, b, pH, lambda, 1);
  x = p;
end
figure (1);
II = x;
GG = chi2;
HH = R;
```

3. Regularized error calculations

```
% This is the objective function for regularization calculation
function [II, G, HH, GG] =fast_regularized_error (p, pKs, A, b, pH, lambda, flag);
[n, m]=size (p); s= p (1:m-1); so = p ( m); s=[0 0 0 s 0 0 0];
q=A*s' + so; bsd=ones (size (b));
% plot it if flag = 1
if flag = =1
  figure (1)
  subplot (221); plot(pH, b, 'ko'); hold on; h=plot(pH, q,' k'); set(h, 'linewidth', 1.5); hold
off;
  ymin = min (b) – max (b)*0.1; ymax = max (b) + max (b)*0.1;
  axis ([2.2 11 ymin ymax])
  subplot (222); plot (pKs, s, 'k.', pKs, s, 'k');
   subplot (223); plot (pH, b-q, 'k.'); axis([3 10.2 -0.02 0.02])
end
% now calculate the error
err = sum ( ( (q-b)./bsd).^2);
% now calculate regularizing function
R = 0; [n ,m] = size(s);
for i = 2:m-1
  R = R+(s(i-1)-2*s(i)+s(i+1))^2;
```

```
end
% Now final error to output
II = log10(err + lambda*R);
G = -1;
HH = err;
GG = R;
```

D. Determination of lambda

```
function [ II, HH, GG, QQ] = search_for_best_lambda (pH, b, maxpH, minpH, pKs, Lts,
So);
% Now sort it
[Y, I] = sort (pH);
for i = 1:size (pH, 1)
  data (i, 1) = pH(I(i));
  data(i,2) = b(I(i),1);
end
pH = data(:,1); b = data(:,2); c = 0;
for i =1:size (pH, 1)
   if pH (i) <= maxpH
      if pH (i) >= minpH
         c = c+1;
         pHs (c) = pH (i);
         bs(c) = b(i);
```

```
    end
  end
end
pH = pHs'; b = bs';
p = [Lts' So];
lambda = 0;
% The best fit without regularization
[Lts_0, chi2_0, R_0] = regularized_fitting (pH, b, pKs, p, lambda, 1); pause (1)
[Lts_0, chi2_0, R_0] = regularized_fitting (pH, b, pKs, p, lambda, 0); p=Lts_0;
[Lts_0, chi2_0, R_0] = regularized_fitting (pH, b, pKs, p, lambda, 1);
Origin = [chi2_0, 0];
II = pH;
HH = b;
GG = origin;
QQ = [Lts_0];
```

E.Optimum lambda

```
function [II, G] = minimize_distance(lambda, p, pH, b, origin, pKs)
[Lts, chi2, R] = regularized_fitting (pH, b, pKs, p, lambda, 0); p = Lts;
[Lts, chi2, R] = regularized_fitting (pH, b, pKs, p, lambda, 1); pause (1);
point = [chi2, R];
distance = sqrt (sum ((origin- point).^2));
II = distance; G = Lts;
```

Appendix B

List of Symbols

θ	Langmuir equilibrium adsorption constant in L/meq of Cd^{2+}
η	Freundlich constant related to adsorption capacity
$[H^+]$	Concentration of proton in mmol/L
$[HL]$	Concentration of site-proton complex in mmol/L
$[L^-]$	Concentration of free site in mmol/g
$[L_T]$	Total Concentration of site in mmol/g
$[M^{2+}]$	Concentration of divalent cation in mmol/L
A	Matrix representing degree of dissociation
$b_{measured}$	Charge excess in mol/g
b_{cal}	Charge excess calculated using model in mol/g
B	Concentration of biosorbent materials in g/L
C_b	Concentration of base in mmol/L
C_a	Concentration of acid in mmol/L
Co	Initial concentration in meq of Cd^{2+}/L
Cc	Concentration of stock solution in meq of Cd^{2+}/L
Ce	Final concentration in meq of Cd^{2+}/L
C_i	Final concentration at of each addition of stock solution (v_i) in meq of Cd^{2+}/L

$k_{1,ads}$	First-order rate constant in min^{-1}
i	i^{th} addition of titrant or stock solution
$k_{2,ads}$	Second-order rate constant in g/meq-min
K_{CH}	Proton binding constant in L/mmol
k_f	Freundlich constant related to intensity
K_{LM}	Metal binding constant in L/mmol
m	Total number of binding sites
n	Total number of titration data points
p	Number of data points
q	Metal uptake in meq of Cd^{2+}/L
qe	Equilibrium metal uptake in meq of Cd^{2+}/L
q_{max}	Maximum metal uptake in meq of Cd^{2+}/Li
So	Added term to account for positive charges in mol/g
SS	Sum of squares for nonlinear regression
SSP	Sum of Squared errors
R	Regularization function
t	Time interval in min
u	Drawing volume of suspension in Liters (L)
V	Volume of suspension in L
W	Weight of biosorbent material in g
X	Vector of unknown sites concentration (L_T)
λ	Regularization strength parameter

Appendix C

$CdCl_2$ Speciation Diagram

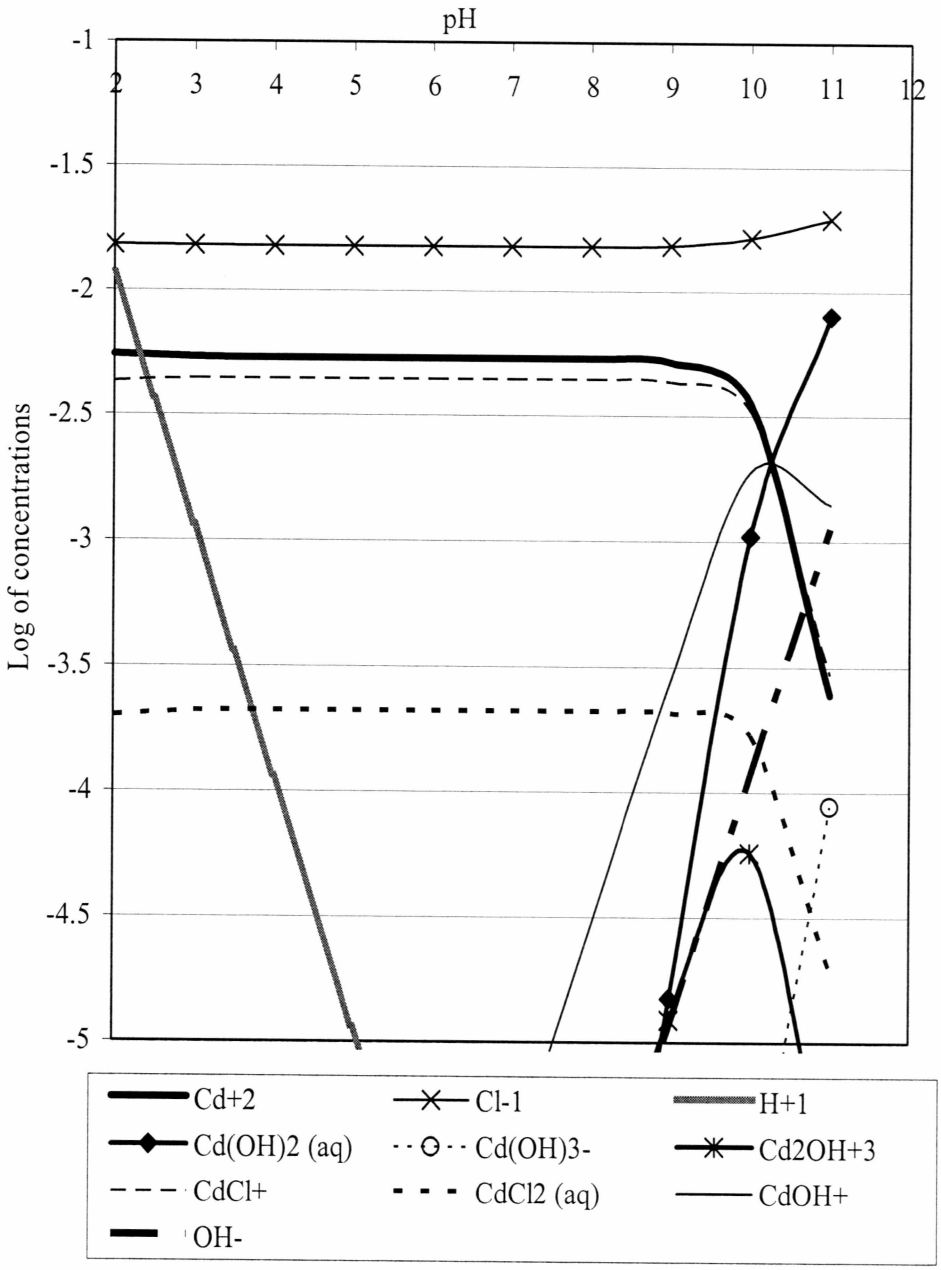

Figure C-1: $CdCl_2$ speciation diagram at pH 5